Ore Geology Reviews 139 (2021) 104541

Contents lists available at ScienceDirect

Ore Geology Reviews

journal homepage: www.elsevier.com/locate/oregeorev

Intrusion-hosted gold deposits of the southeastern East Sayan (northern Central Asian Orogenic Belt, Russia)

Bulat B. Damdinov [a,*], Xiao-Wen Huang [b], Nikolay A. Goryachev [c,d], Sergey M. Zhmodik [e], Anatoly G. Mironov [a], Ludmila B. Damdinova [a], Valentin B. Khubanov [a], Vadim N. Reutsky [e], Denis S. Yudin [e], Alexey V. Travin [e], Viktor F. Posokhov [a]

[a] Geological Institute, Siberian Branch of the Russian Academy of Sciences (GIN SB RAS), 6a, Sakh'yanovoi Str., Ulan-Ude 670047, Russia
[b] State Key Laboratory of Ore Deposit Geochemistry, Institute of Geochemistry, Chinese Academy of Sciences, 99 West Lincheng Road, Guiyang 550081, China
[c] North-East Interdisciplinary Scientific Research Institute, Far East Branch of the Russian Academy of Sciences (NEISRI FEB RAS), 16 Portovaya Str., Magadan 685000, Russia
[d] Institute of Geochemistry, Siberian Branch of the Russian Academy of Sciences (IGC SB RAS), 1a Favorskogo Str., Irkutsk 664033, Russia
[e] Institute of Geology and Mineralogy, Siberian Branch of the Russian Academy of Sciences (IGM SB RAS), 3 Ak. Kotyuga Ave., Novosibirsk 630090, Russia

ARTICLE INFO

Keywords:
Southeastern East Sayan
Altaid Belt
Russia
Intrusion-hosted gold deposits
Isotopes
Age
Tectonic setting

ABSTRACT

Our paper reviews a series of relatively low-grade gold deposits and prospects hosted by granitoid intrusions within the southeastern East Sayan in the Altaid Belt (northern Central Asian Orogenic Belt, Russia). The studied deposits/prospects are characterized by the presence of Te-, Sb- and Bi-bearing minerals. However, they differ in their main gold-associated mineral assemblages, which permits to distinguishing four mineralization assemblages: 1) gold-telluride; 2) gold-tetradymite; 3) gold-stibnite; and 4) gold-bismuth sulfosalt. The gold-telluride mineralization (1) is represented by the Tainskoye deposit, and the Khoringolskoye and Sagangolskoye prospects which are defined by paragenesis of native gold with Au-Ag-Bi-Pb-Ni tellurides, such as hessite, petzite, altaite, wehrlite, calaverite, melonite, altaite, and tellurobismuthite. The gold-tetradymite mineralization (2) which is represented by the Konevinskoye deposit, is hosted by the Saylag granitoid pluton, and contains tetradymite as one of the principal minerals associated with native gold. The gold-stibnite mineralization (3), represented by the Tumannoye prospect, is also hosted in a granitoid complex consisting of granodiorite and leucogranite. The gold-bismuth-sulfosalt mineralization (4) is documented at the Pogranichnoye prospect, where native gold is associated with the bismuth-bearing minerals: bismuthinite, galeno-bismuthite, lillianite, and native bismuth. Estimated $\delta^{18}O$ values of ore-forming fluids from intrusion-hosted deposits range from 5.7 to 7.4‰, indicative of a magmatic origin; $\delta^{34}S$ values of sulfides vary from −4.2 to 4.5‰, which corresponds to magmatic sulfur. The geological setting, element geochemistry of host granitoids, stable isotope ratios, and mineralogy of the studied deposits are consistent with a magmatic origin of the mineralizing fluids.

The studied deposits are spatially associated with either Neoproterozoic or Early Paleozoic granitoids, belonging to the two main orogenic stages of the East Sayan geodynamic evolution. At ~850 Ma, during the Neoproterozoic stage, deposits with dominant gold-telluride assemblages, formed in association with granitoids characterized by geochemical features of island arc granites. During 458–439 Ma, in the Early Paleozoic stage, gold-tetradymite, gold-stibnite, gold-telluride and gold-bismuth-sulfosalt assemblages were formed that are spatially associated with orogenic granites with different geochemical compositions. Most gold-bearing mineral assemblages are intersected by post-mineral Late Paleozoic dykes. The origin of these different gold-sulfide-telluride assemblages is explained with their genetic association with granitoid intrusions of different ages and compositions.

* Corresponding author.
E-mail address: damdinov@mail.ru (B.B. Damdinov).

https://doi.org/10.1016/j.oregeorev.2021.104541
Received 26 March 2021; Received in revised form 19 October 2021; Accepted 20 October 2021
Available online 25 October 2021

1. Introduction

Intrusion-related gold mineralization often occurs as large but low-grade deposits of potential economic interest (Goldfarb et al., 2005; Seedorff et al., 2005; Sillitoe, 2000; Sillitoe and Thompson, 1998; Vikent'eva et al., 2018). Such mineralization permits the study of magmatic-hydrothermal systems and element association behaviors in magmatic and hydrothermal processes. Our study aims to elucidate the key factors controlling the enrichment of gold and other metals at the intrusion-hosted gold deposits of the southeastern East Sayan. Comprehensive study of such mineralization has both theoretical and practical value.

Some gold deposits, hosted within granite plutons, are characterized by the Te-Bi-As-Sb association (Hart, 2007; Maloof et al., 2001). Most of them have a direct genetic relationship with their magmatic host rocks. Such gold deposits are widespread in a broad range of regimes, from supra-subduction, to intraplate and collision settings (Gao et al., 2018; Hart et al., 2002; Mao et al. 2014; Seedorff et al., 2005; Sillitoe, 2000; Sillitoe and Thompson, 1998; Vikent'eva et al., 2018).

A number of smaller gold deposits and prospects, spatially associated with granitoid intrusions, are known in the southeastern East Sayan (Altaid Belt, northern Central Asian Orogenic Belt, Russia). These occur as gold-quartz veinlets and gold-sulfide zones hosted within granitoids. They differ from the major orogenic gold deposits of the same region in their geological setting, ore mineral assemblages, and isotopic composition. Moreover, they also differ from each other in their mineralogy. In this paper, we present a review of the intrusion-hosted/related gold deposits and prospects of this region, based on previously published and new data on deposit geology, ore composition, age, fluid inclusion, and S-O isotopes. Our aim is to providing a better insight into the origin of intrusion-hosted gold deposits and the controlling factors on the origin and compositional variations of the gold mineralization as well as proposing a geological model for the formation of the granitic host intrusions.

2. Geology and gold metallogeny of the southeastern East Sayan

The southeastern East Sayan is a part of the Altaid Belt located in the northern part of the Central Asian Orogenic Belt (Fig. 1). Geographically, this region is situated near Lake Baikal and is a part of the Republic of Buryatia, Russia. The studied region is located at the southern margin of the Siberian Craton and is characterized by a complex geological evolution (Fig. 2). The area consists of genetically different tectonic blocks, which include the northern part of the Tuva-Mongolian microcontinent, the Oka accretion prism, the Dunzhugur, Sarkhoy, and Shishkhid island- and continental-arc rock assemblages (Kuzmichev, 2015). The southeastern East Sayan is characterized by widespread cover (thrust) and fold structures. Features of the regional geological structure have been published in research papers and monographs (Dobretsov, 1985; Fedotova and Khain, 2002; Kuzmichev, 2015; Zhmodik et al., 2008).

The Tuva-Mongolian microcontinent is composed of Archean basement and Neoproterozoic cover. The Archean basement is represented by several blocks (see Fig. 2) consisting of gneisses, with minor amphibolites and migmatites. The published age of the Archean basement is 2.7 Ga (Anisimova et al., 2009). The Neoproterozoic cover consists mainly of carbonate strata with minor terrigenous rocks, the age of which was determined as 1250–540 Ma (Kuznetsov et al., 2010). Probably a part of the sedimentary rocks could be formed at Mesoproterozoic. The Oka accretion prism is represented by metamorphosed volcanic rocks (Oka series) composed of amphibolites and green schists, including narrow zones of blueschists (Kuzmichev, 2015). Rocks of the Oka accretion prism have an age of 736–753 Ma (Kuzmichev, 2015).

The Dunzhugar ophiolites, which are located on the outer margin of the Archean basement Gargan block, have been dated at more than 1020 Ma, making them the most ancient in the Central Asian Fold Belt (Khain et al., 2002). These ophiolite rocks represent relics of an island-arc rock assemblage of the same name. The continuation of the Shishkhid ophiolite belt stretches along the whole northern edge of the Oka

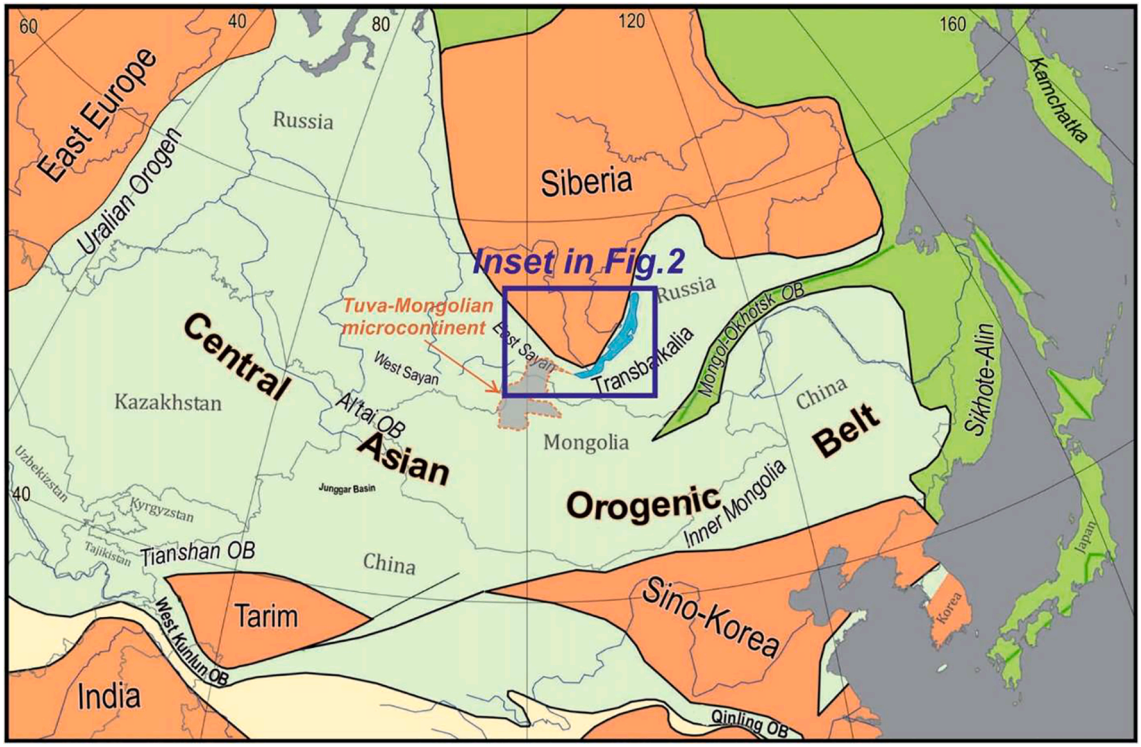

Fig. 1. General map of the Central Asian Orogenic Belt and the studied area location (adapted from Safonova & Santosh, 2014). Filled areas: cratonic blocks (red); orogenic belts (gray, green, and light-yellow) formed after the closure of the Paleoasian, Pacific, and Thetyan oceans, respectively. Contours of the Tuva-Mongolian microcontinent after (Kuzmichev, 2015). (For interpretation of the references to colour in this figure legend, the reader is referred to the web version of this article.)

Fig. 2. Simplified geological and metallogenic map of the southeastern part of the East Sayan (based on the Okinskaya geological expedition data).

accretion prism (Kuzmichev et al., 2005). Here, the belt consists of relatively small lens-like ultrabasic and basic rock bodies. Most are too small to be shown at the map scale of Fig. 2. The age of the Shishkhid ophiolites is about 800 Ma (Kuzmichev et al., 2005). The Oka prism and Shishkhid ophiolites together define the Shishkhid island arc (Kuzmichev, 2015).

The Sarkhoy continental arc rock assemblages are represented by the metamorphosed volcanic rocks (Sarkhoy series) included in the Neoproterozoic cover of the Tuva-Mongol microcontinent. The Sarkhoy series rocks age lies within the range of 805–770 Ma, and they outcrop in the western part of the Bokson-Garganskaya metallogenic zone (see Fig. 2.

The Tuva-Mongolian microcontinent borders the Ilchir and the Khamsara terranes, indicated on Fig. 2 as the Ilchirskaya and Khamsarinskaya metallogenic zones, respectively. The tectonic setting of the Ilchir terrain is interpreted as a passive margin of the Paleozoic Dzhida oceanic basin, whereas the Khamsara terrain is probably an Early Paleozoic continental arc of the Tuva-Mongolian microcontinent (Kuzmichev, 2015). The boundaries of the described terranes are represented by major deep faults separating areas of rock assemblages formed in different geodynamic settings.

The rocks of the above-mentioned blocks are cut by numerous intrusions of gabbro-plagiogranite, gabbro-syenite, and leucogranite associations as well as by numerous dyke series, although these magmatic rocks of the region are less studied. There is some uncertainty about the evolution of granitoid magmatism due to insufficient geochronological data and partially to relatively small amounts of paleontologically characterized host strata. The Neoproterozoic Sumsunur intrusive granitoid series are considered the oldest plutonic rocks. The relatively widespread Paleozoic intrusions are represented by the Khoitooka (gabbroid), Khuzhirtai-Gorkhon (gabbro–syenite), Tannuol (tonalite–granodiorite), Urik and Sarkhoi (granite), and Ognite and Botogol (alkaline) magmatic series. Frequently encountered small intrusions (dikes, sills) are defined as the Oka, Kholba, Barun–Kholba, and Ilei

subvolcanic series. However, in most cases, there is no information on the dike ages. Younger magmatism consists of Cenozoic basalts.

The Neoproterozoic and Paleozoic tectonic evolution of the southeastern East Sayan is described in a number of publications (Gordienko et. al., 2016; Kuzmichev, 2015; Zhmodik et al., 2006). Several geodynamic stages were determined: oceanic, island arc, accretionary-collisional, rifted (Kuzmichev, 2015; Zhmodik et al., 2006; Buslov, 2011; Fedotova and Khain, 2002, et al.). These stages indicate the existence of terranes, composed of rock assemblages that formed in the corresponding geodynamic settings.

The oldest rocks of the region are represented by outcrops of Archean basement of the Tuva-Mongolian microcontinent (e.g. Gargan Block). However, the lack of available information on these rocks hampers an understanding of the Archean evolution of the region.

The earliest reliably established stage of the East Sayan Fold Belt is the opening of the Paleoasian Ocean (Gordienko et al., 2016; Yarmolyuk et al., 2006), which was accompanied by the formation of the Dunzhugur ensimatic island arc, that has been estimated as being older than 1035–1022 Ma (Khain et al., 2002). The Dunzhugur island arc continued to be periodically active until around 810 Ma when it collided with the passive margin of the continental Gargan Block. During this period, the island arc system was accompanied by granitoid magmatism, fragments of which are observed in the ophiolite allochthons as small bodies of island arc granitoids. The isotopic age of one of these, the Tainsky pluton, has been determined as 853 Ma (Damdinov et al., 2020b).

Later, at about 800 Ma, following the collision with the Gargan continental block, the Dunzhugur ophiolites were obducted as a thrust sheet covering much of that Archean basement block. Subsequently, the convergent tectonic regime switched to subduction below the continental block and, with the formation of a continental margin arc, represented by the Sarkhoy volcanic arc. This continental arc characterized much of the period from 800 to 500 Ma (Kuzmichev, 2015).

Early Paleozoic granitoids in the adjacent regions of Tuva and Northern Mongolia indicate island arc magmatism was active until around 520–510 Ma. Subsequently, from 500 Ma, the character of magmatism changed with formation of late orogenic granitoids (Rudnev et al., 2015). Therefore, it is suggested that late-orogenic post-subduction stage commenced at about 500 Ma ago (Damdinov et al., 2018; Gordienko et al., 2016). The late orogenic events continued during a period of 500–420 Ma (Damdinov et al., 2018). After this stage, a continental regime settled in the region.

In the Late Paleozoic, the studied area, as well as the bulk of the Central Asian Fold Belt, underwent intense strike-slip deformation, defining a Late Paleozoic strike-slip stage of the tectonic evolution at 380–285 Ma (Buslov, 2011). The large-scale strike-slip deformations within the bulk of the Central Asian Fold Belt were caused by the collision of the Siberian and Kazakh-Baikal continents, which resulted in the formation of the North Asian craton. The craton later collided with the East European continent (Buslov, 2011).

The period from the Mesozoic to the Cenozoic is not reflected in the tectonic evolution of the East Sayan due to the absence of Mesozoic rocks. In the Cenozoic, intraplate basalt magmatism occurred (Yarmolyuk et al., 2003).

The region studied falls within the Oka ore district (see Fig. 2 that consists of four different metallogenic belts (Gordienko et al., 2016; Damdinov, 2019), the boundaries of which coincide to the terrane borders discussed above. The metallogenic zones (Ilchirskaya, Bokson-Garganskaya, Okinskaya, and Khamsarinskaya) host zones and clusters gold deposits and prospects. Within the latter, there are some economic gold deposits and numerous gold prospects (see Fig. 2). The largest economic orogenic gold deposits (Zun-Kholba, Zun-Ospa, etc.) are concentrated at the margins of the Gargan block (a fragment of the Tuva-Mongolian microcontinent's Archaean basement). This area is identified as the Urik–Kitoyskaya gold zone and includes the Gargansky, Ulzytinsky, Uriksky, and Kholbinsky gold clusters. In the east, the Urik-Kitoyskaya gold zone borders on the Olginskaya gold zone. Individual gold clusters are known in addition to the gold zones. The Tissa–Sarkhoisky gold cluster is situated in the westernmost part of the studied region; the Dibinsky gold cluster, in its southern part; and the Ospinsky gold cluster, in the eastern part of the researched area. The Ospinsky gold cluster is spatially associated with the Ospa–Kitoi ultrabasic ophiolitic massif and its nearest margin.

The studied intrusion-hosted gold deposits and prospects are spatially scattered throughout the region (see Fig. 2. The economic intrusion-hosted gold deposits are the Konevinskoye and Tainskoye, containing high average gold contents of 11.6 and 24.1 ppm, but relatively small total reserves of about 14 and 10 tons, respectively. Other gold occurrences in the area are low-grade or unexplored prospects, the largest of which are described in this paper.

3. Analytical methods

The paper is based on previously published data with addition of new results obtained by using the analytical methods presented below. Most of the analyses were conducted with the use of facilities at the Common Use Analytical Center for the Analytical Center of Mineralogical, Geochemical, and Isotope Studies, of the Geological Institute, SB RAS, Ulan-Ude, Russia.

Oxygen isotopes in silicates (quartz and muscovite) were analyzed using laser fluorination. All measurements were carried out on a Finnigan MAT 253 mass spectrometer using a double inlet system for oxygen in silicates. The measurements were calibrated using international standards NBS-28 (quartz), NBS-30 (biotite) (Coplen, 1988) for silicates. The error of the obtained values is less than 0.2–0.3‰.

Laser ablation for U-Pb zircon dating was conducted using an UP-213 (New Wave Research) laser ablation system. The isotope analysis of a laser-vaporized zircon substance was performed on a Thermo Scientific Element XR single collector sector-field ICP mass spectrometer. The detailed description of the analytical technique and parameters of the procedure were published in Khubanov et al. (2016). The analyzed zircon grains were separated from altered host granites only.

Fluid inclusions (FI) in quartz were investigated by thermometry and cryometry. To determine the homogenization temperature, eutectic temperature and ice melting temperature of aqueous solutions, temperatures of dissolution of daughter phases, a Linkam THMSG-600 microthermocamera with temperature range from −196 to +600 °C was used. The standard instrumental measurement error is ±0.1 in the negative and ±5 °C in the positive temperature range. The bulk salinity of the solutions (eq. NaCl) was determined by cryometry data, according to Bodnar and Vityk (1994). The salt composition was identified based on the eutectic temperature of the fluid using the data by Borisenko (1977).

Chemical compositions of ore minerals were analyzed using a LEO-1430 scanning electronic microscope with an attached INCA-Energy energy-dispersion device for quantitative analysis.

The sulfur isotopic ratios were determined on a mass-spectrometer (Finnigan MAT Delta dual inlet mode) at the Common Use Center for Multi-Element and Isotopic Research of IGM SB RAS, Novosibirsk, Russia. The isotopic composition of the sulfur is expressed as a $\delta^{34}S$ unit, in permil (‰), relative to the Canyon Diablo Troilite standard, and its analytical precision is about ±0.2‰.

A $^{40}Ar/^{39}Ar$ isotope analysis was carried out at the Center for Collective Use of Multi-Element and Isotope Studies of the Institute of Geology and Mineralogy of the Siberian Branch of the Russian Academy of Sciences (Novosibirsk, Russia) using the step heating method according to the previously published technique (Travin et al., 2009). Samples, together with MCA-11 muscovite (age – 311.0 ± 1.5 Ma) used as a monitor and calibrated with the help of international standard samples of LP-6 biotite and Bern-4 m muscovite, were wrapped in aluminum foil, placed in a quartz ampoule, and vacuum-sealed. Then, the samples were irradiated in the cadmium channel of a scientific reactor at the BBP-Ktype at the Physics and Technology Institute of Tomsk Polytechnic

University (Tomsk, Russia). The neutron flux gradient did not exceed 0.5% in the sample size. Step heating experiments were carried out in a quartz reactor with an external heating furnace, the blank testing defining ^{40}Ar (10 min at 1200 °C) did not exceed 5×10^{-10}ncm^3. Argon was purified by using ZrAl-SAES getters. The isotopic composition of argon was measured with the help of a Noble gas 5400 mass spectrometer produced by Micromass (England). The measurement errors correspond to the interval of ±1 σ. The following coefficients were used to correct interfering argon isotopes formed during irradiation on Ca, Cl, K: $(^{39}Ar/^{37}Ar)_{Ca} = 0.000891 \pm 0.000003$, $(^{36}Ar/^{37}Ar)_{Ca} = 0.000446 \pm 0.000004$, $(^{40}Ar/^{39}Ar)_K = 0.089 \pm 0.001$. Before measuring, preliminary degassing of the samples was carried out at temperature 350 °C. To control the isotope discrimination of the mass spectrometer, portions of purified atmospheric argon were regularly measured. The average value of the ratio $^{40}Ar/^{36}Ar$ for the measurement period was 299 ± 1. When interpreting the age and Ca/K spectra, we used the age plateau method, which implies calculating the average weighted age for several (at least three) consecutive temperature steps with consistent age values close to Ca/K ratios. The share of allocated ^{39}Ar corresponding to the plateau should be at least 50%.

Re-Os dating was performed at the State Key Laboratory of Ore Deposit Geochemistry, Institute of Geochemistry, Chinese Academy of Sciences (Guiyang, China), on an ELAN DRC-e inductively coupled plasma-mass spectrometry (ICP-MS) instrument. Approximately 10 mg of concentrated molybdenite was weighed and loaded into a 120-ml reusable Carius tube with known amounts of ^{185}Re and ^{190}Os spikes. The samples were then digested and equilibrated using 10 ml of concentrated HNO_3 and 2 ml HCl. The tube was subsequently placed in a stainless-steel jacket and heated at 200 °C for about 12 h. After cooling, Os was separated from the matrix as OsO_4, using the *in situ* distillation equipment, and Re was extracted from the remaining solution utilizing an anion exchange resin (Biorad AG 1-X8, 200–400 mesh). More detailed procedure was described in Hunger et al. (2018).

K/Ar dating was carried out at the North-East Integrated Scientific Research Institute of the Far-East Branch of the Russian Academy of Sciences (Magadan, Russia). A potassium analysis was done by atomic absorption spectroscopy on an AAS-1 spectrometer. Argon isotopes were measured on an improved MI-1201 IG mass spectrometer using a reconstructed metal melting reactor, and glass vacuum tubes were used for extracting radiogenic ^{40}Ar, ^{36}Ar, and ^{38}Ar spike with lower detection limit around 0.5–1 ng. Geo-reference samples MSA-11 and MSA-12 (Russian Academy of Sciences' Inter-Laboratory Standards, 290 Ma) were repeatedly measured to control accuracy and precision of the analytical procedure, giving uncertainties of <1% for potassium and <2–5% for argon. The age errors are estimated as <2% for 75% of the measurements.

4. Species of the intrusion-hosted gold deposits

The intrusion-hosted gold deposits and prospects of the southeastern East Sayan are hosted in different granitoid types and occur in a number of different metallogenic zones. The main metallic minerals in all of the deposits/prospects studied are pyrite or arsenopyrite, with minor pyrrhotite and base metal sulfides (chalcopyrite, galena, sphalerite). The only differences observed are in the gold-bearing mineral assemblages, four of which have been recognized, namely: gold-telluride, gold-tetradymite, gold-stibnite, gold-bismuth-sulfosalt. These are interpreted to reflect geochemical characteristics of gold mineralization in the different species of the studied intrusion-hosted deposits/prospects.

4.1. Gold-telluride mineralization

The Tainskoe deposit as well as the Khoringolskoe and Sagangolskoe prospects are the largest of those characterized by the gold-telluride assemblage. They are spatially associated with Neoproterozoic and Early Paleozoic island arc plagiogranites and granodiorites. The ore mineralization of these deposits and prospects are characterized by the widespread gold-telluride association including native gold with tellurides of gold, silver, bismuth, and lead. The tellurides are hessite, petzite, altaite, wehrlite, calaverite, melonite, altaite, and tellurobismuthite. All tellurides formed at the latest stages of ore formation.

4.1.1. Tainskoye deposit (Fig. 2, No. 1)

The Tainskoye deposit is located in the Neoproterozoic Tainsky granodiorite and plagiogranite pluton (Damdinov et al., 2020b; Mironov et al., 2001). This 300 × 700 m pluton intrudes serpentinites and serpentinized harzburgites of the Ospa-Kitoy ophiolite ultramafic massif (Fig. 3). Coeval granitoids and ophiolites consist of a single allochthon cover thrust over the Archean basement of the Tuva-Mongolian microcontinent (Fig. 4a). U-Pb dating of zircons from the Tainsky pluton, hosting the Tainskoe gold deposit, yields the age of **853 ± 10** Ma (Fig. 5a, Damdinov et al., 2020b). Similar ages were obtained by $^{40}Ar/^{39}Ar$ (**855.8 ± 5.1** Ma) dating of hornblende (Damdinov et al., 2020b) and Re-Os (**860** Ma) dating of molybdenite (Mironov et al., 2005). This Neoproterozoic age corresponds to the late stage of the Dunzhugur island arc (Paleoasian ocean).

The Tainskoye granitoids have a moderate SiO_2 content of 61–65 wt %. All rocks have sodium geochemical specialization where the K/Na ratio varies from 0.08 to 0.82 with an average value of 0.33. Trace elements show low content of incompatible elements according to the upper crust (Rudnick and Gao, 2003) normalized spider diagram (Fig. 6a). The granitoids curves show positive Ba, Sr and negative U, Th, Zr, Hf, Pb anomalies. Chondrite normalized (Sun and McDonough, 1989) rare-earth element patterns are characterized by LREE enrichment ($La/Yb_n = 8.8–12.8$) with no specific anomalies for any elements (Fig. 6b). The geochemical data allow the suggestion that the Tainsky granitiods are of an island arc origin (Damdinov et al., 2020b). Ore-hosting granitoids are often cataclased and mylonitized as well as quartz-sericite altered, with minor carbon and sulfide alteration.

There are three types of mineralization: low-sulfide quartz veins, quartz-muscovite-pyrrhotite zones, and veinlet-disseminated. All types are hosted in the granitoid pluton and do not persist beyond its margin (see Fig. 3). Quartz veins are characterized by gray crystalline quartz with nest-impregnated sulfide mineralization (Fig. 4b). Most telluride minerals occur in quartz lodes. Quartz-muscovite-pyrrhotite ores are characterized by high sulfide content (60–70 modal% pyrrhotite) associated with grainy light-gray and white quartz and muscovite. The veinlet-disseminated type of ore is zones of quartz veinlets and sulfide impregnation in altered plagiogranites. The main ore minerals of this deposit are pyrrhotite, galena, sphalerite, chalcopyrite, and pyrite (Fig. 4c). There are also tellurides, including hessite, wehrlite, and altaite associated with argentite, native gold, and silver. Native gold in the Tainskoye ores shows significant variations in fineness (Fig. 4d). Gold-silver minerals are represented by varieties from native silver to high-grade gold (fineness up to 999‰).

According to Mironov et al. (2001), the homogenization temperatures of fluid inclusion in quartz show that different ore mineral associations were deposited with decreasing temperature from more than 400 °C for veinlet-disseminated ores to more than 165 °C for telluride-bearing quartz veins. Quartz-muscovite-pyrrhotite ores formed at the minimal temperature of about 270 °C. The pressure of mineral formation decreased from 950 to 130 bar. Dominating in the fluid salt systems are $CaCl_2 + NaCl + KCl + H_2O$, with minor admixtures of Li, Zn, and Fe chlorides.

The measured isotope values are presented in Table 1. $\delta^{34}S$ values of the Tainskoye sulfides vary from 3.1 to 4.5 ‰. The calculation of formation temperature for the two pyrrhotite-chalcopyrite pairs by the isotopic geothermometer (Li and Liu, 2006) shows a consistent value of 359 °C (Table 1, Samples Tn-11 and Tn-458). The calculated isotopic composition of sulfur in H_2S of the ore-forming fluid is 2.6 – 4.4‰ for this temperature (359 °C). The oxygen isotopic composition of lode quartz is 13.2–13.3‰. The calculation of the oxygen isotopic

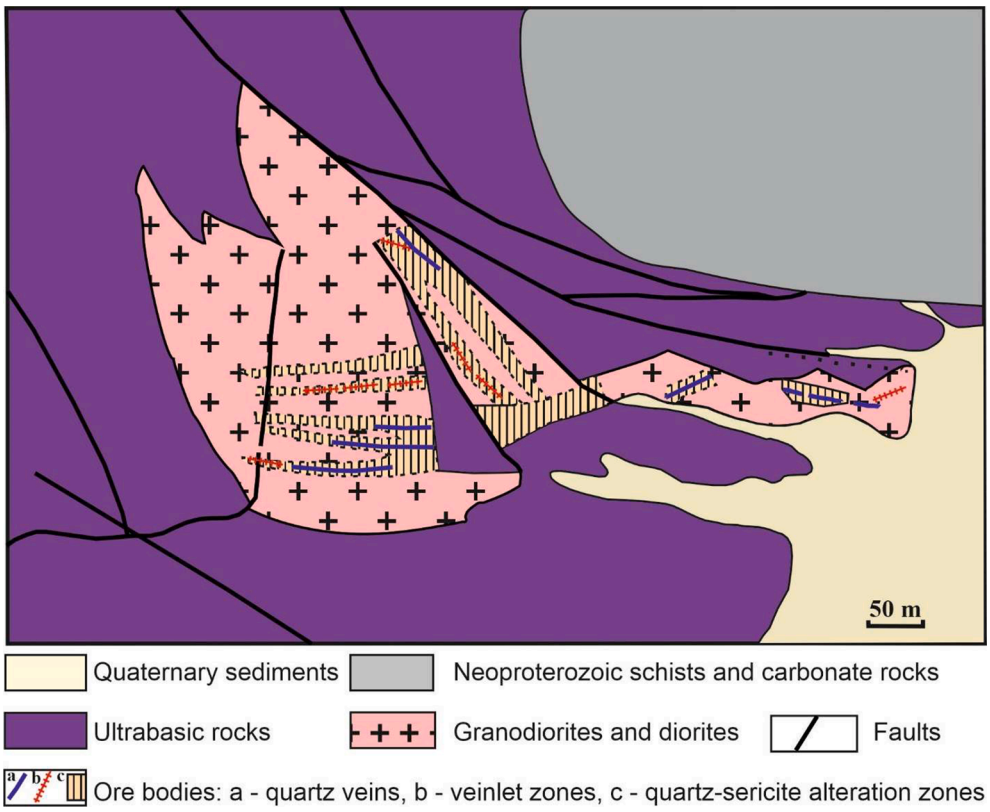

Fig. 3. Geological map of the Tainskoye gold deposit (after Mironov et al., 2001).

composition in the equilibrium fluid for the temperature of 359 °C yields $\delta^{18}O$ values of 8.0 – 8.1‰ corresponding to the magmatic oxygen isotope ratio values (6 – 10‰, Hoefs, 2009).

4.1.2. Khoringolskoye and Sagangolskoye prospects (Fig. 2, No. 2)

Both prospects are located in granitoid intrusions cutting through Neoproterozoic metamorphosed effusive rocks of the Sarkhoy series and Neoproterozoic metamorphic rocks (schists, amphibolites) (Fig. 7; Damdinov et al., 2007). Coarse-grained plagiogranite hosting the Sagangolskoye prospect has a zircon U-Pb age of **499 ± 6** Ma (Fig. 5b). $^{40}Ar/^{39}Ar$ dating of sericite from wall-rock quartz-sericite metasomatites yields the similar isotopic age of **482.3 ± 5.3** Ma (Fig. 8a). Previous Rb-Sr dating of the bulk of the near-lode quartz-sericite metasomatites (berezites) from diffusion rims showed an age of **537 ± 15** Ma (Damdinov et al., 2007). This date is not entirely accurate but nevertheless reflects the Early Paleozoic age of the mineralization.

Host ore granitoids are represented by plagiogranites and granodiorites. These rocks have SiO_2 contents of 62.3 – 71.5 wt% and K/Na ratios of 0.17 – 1.09 with the average value of 0.48. The granitoids have Ba, Sr positive anomalies and weakly negative Th, U, Nb, Zr anomalies at the upper crust normalized spider diagram (Fig. 9a). Fractionation of REE is not obvious, with slight LREE enrichment (La/Yb_n = 4.2 – 16.5; Fig. 9b). Geochemical features of the Khoringolskoye and Sagangolskoye granitoids correspond to those of the Tainskoye granitoid pluton and are similar to those of island arc granites.

Mineralization zones are represented by low-sulfide quartz veins with near-lode quartz-sericite rims, zones of quartz veinlets (stockwork), and disseminated pyrite zones in plagiogranites (Fig. 10a-b). Pyrite is the main ore mineral. There are minor amounts of chalcopyrite, pyrrhotite, galena, and native gold as well as rare chalcocite and molybdenite. The tellurides, including calaverite, hessite, petzite, melonite, altaite, and tellurobismuthite, are associated with native gold. Distinguished in the ore mineralization are two mineral associations: gold-pyrite and gold-telluride (Fig. 10c-e). The gold-telluride association formed at the late stage of ore mineral formation. Native gold fineness varies from 822 to 999‰. Gold fineness distribution lies within the modal value interval between 900 and 950‰. Gold content of ores vary widely from 0.02 to 52.4 ppm, with an average grade about 3.36 ppm. Tellurium content in ores range up 3 to 51 ppm.

According to (Damdinov et al. 2007), two types of fluid inclusions in gold-bearing quartz with high (>325 – 250 °C) and low (175 – 130 °C) homogenization temperatures reflecting different ore mineral associations have been determined. Moreover, some small crystal-fluid inclusions are present in the quartz growth zones. Due to the extremely small size of the former, it was impossible to study them. High-temperature fluid inclusions decrepitate at 325 °C. Measured fluid inclusion (FI) homogenization temperatures of low-temperature inclusions reflect minimal temperatures of fluid inclusion trapping; therefore, the host mineral formation temperature has to be higher. According to the Au-Ag-Te stability diagram (Bortnikov et al., 1988), the gold-telluride association is stable at 280 °C. The bulk salinity of fluids is 4.0 – 11.7 wt% eq. NaCl, sodium chloride prevails in the salt composition.

The sulfur isotope composition of sulfides is highly various (−4.2 to 4.3‰; see Table 1). The calculation of the isotopic composition of sulfur in H_2S in the equilibrated fluids for temperature of 300 °C (possible temperature for quartz and pyrite formation) shows predominantly near-zero values, but in some cases negative $\delta^{34}S$ values (-3.3 to −5.4‰) were observed. In various granitoid bodies, amounts of isotopically "light" sulfur were different, which resulted in some differences in sulfur isotopic compositions in the Khoringolskoye and Sagangolskoye prospects. The oxygen isotope compositions of ore-bearing quartz from the studied prospects are 8.9 – 13.3‰. The calculation of the equilibrium fluid composition for T = 300 °C results in the $\delta^{18}O$ values of 5.7 – 6.3‰. In quartz from the Khoringolskoye prospect, $\delta^{18}O$ values of the fluids are 2.0–4.4‰.

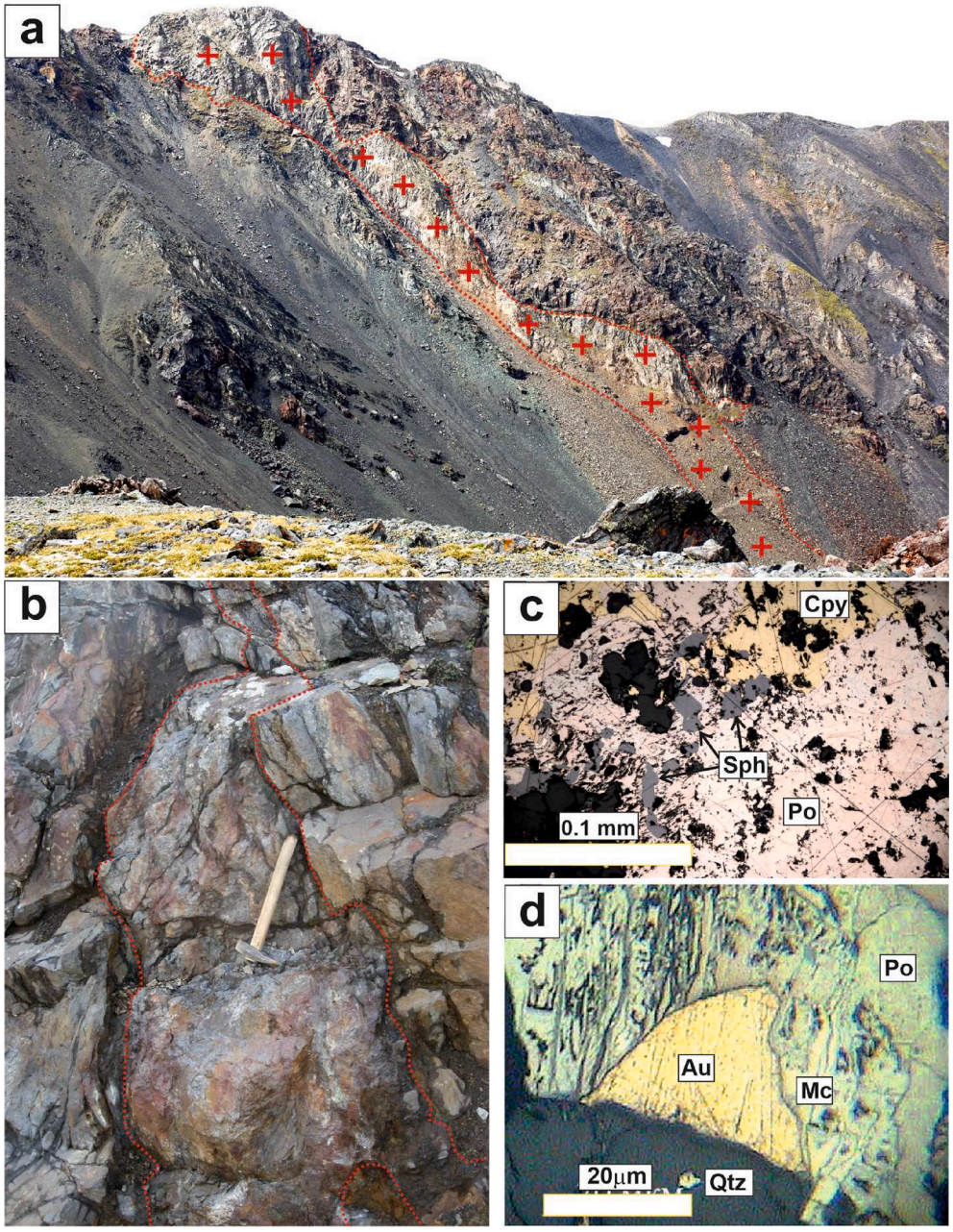

Fig. 4. (a) – photo of the Tainsky granitoid massif (contoured) intruded in ultrabasic rocks of the Ospa-Kitoy ophiolite massif; (b) field photos showing a large quartz vein in grey altered diorites of the Tainskoye deposit; (c) reflected light image showing the main sulfide minerals composed of pyrrhotite, chalcopyrite, and sphalerite; (d) occurrence of a native gold grain in a mineral assemblage of pyrrhotite, partly replaced by marcasite, and quartz. Mineral abbreviations: Qtz – quartz, Po – pyrrhotite, cPy – chalcopyrite, Sph – sphalerite, Au – native gold, Mc – marcasite.

4.2. *Gold-tetradymite mineralization*

The Konevinskoye deposit and surrounding small prospects represents gold mineralization containing the gold-tetradymite assemblage. The similar Obogolskoye gold prospect is in the southwestern part of the studied area (western part of the Tissa-Sarkhoisky ore cluster). All these deposits and prospects are within the Early Paleozoic Tannuol series granitoids.

4.2.1. ***Konevinskoe deposit*** *(Fig. 2, No. 3)*

The deposit is hosted by the Saylag granodiorite pluton (Damdinov et al., 2016) and has a 12 × 7 km oval shape in plan. The pluton is hosted in Neoproterozoic carbonate rocks and, in its western part, in Late Paleozoic metamorphosed effusive rocks (Fig. 11). The Saylag pluton granodiorites, hosting the Konevinskoe gold deposit, have a U-Pb age of **486 ± 4** Ma (see Fig. 5c). Re-Os dating of molybdenite from a gold-bearing quartz-molybdenite-pyrite veinlet yields the model age of **458.5 ± 3.7** Ma (Table 2. Biotite from subvolcanic dykes cutting granitoids has a $^{40}Ar/^{39}Ar$ age of **324 ± 5.3** Ma (Damdinov et al., 2016).

Granitoids of the Saylag pluton are equated with the Early Paleozoic Tannuol intrusive series and represented by biotite- and hornblende-bearing granodiorites. The granitoids have SiO_2 content from 65.6 to 76.4 wt%, with the K/Na ratios varying from 0.64 to 2.24. Trace element spider diagrams show that the granitoids have an upper crust geochemical composition, whereas REE distribution is similar to that of the Tainskoye island arc granitoids, although it has the low contrast Eu minimum (Fig. 12a-b). Such geochemical characteristics of granitoids are similar to continental arc granites (Damdinov et al., 2016).

Granitoids often undergo quartz-sericite, silicic, and K-feldspar alteration. Altered granitoids are enriched in gold, with content ranging from 0.05 to 0.25 ppm, and contain disseminated pyrite and chalcopyrite, whilst those that are weakly altered carry quartz-pyrite-molybdenite veinlets (Fig. 13a). The granitoids are cut by numerous dykes of intermediate to basic composition.

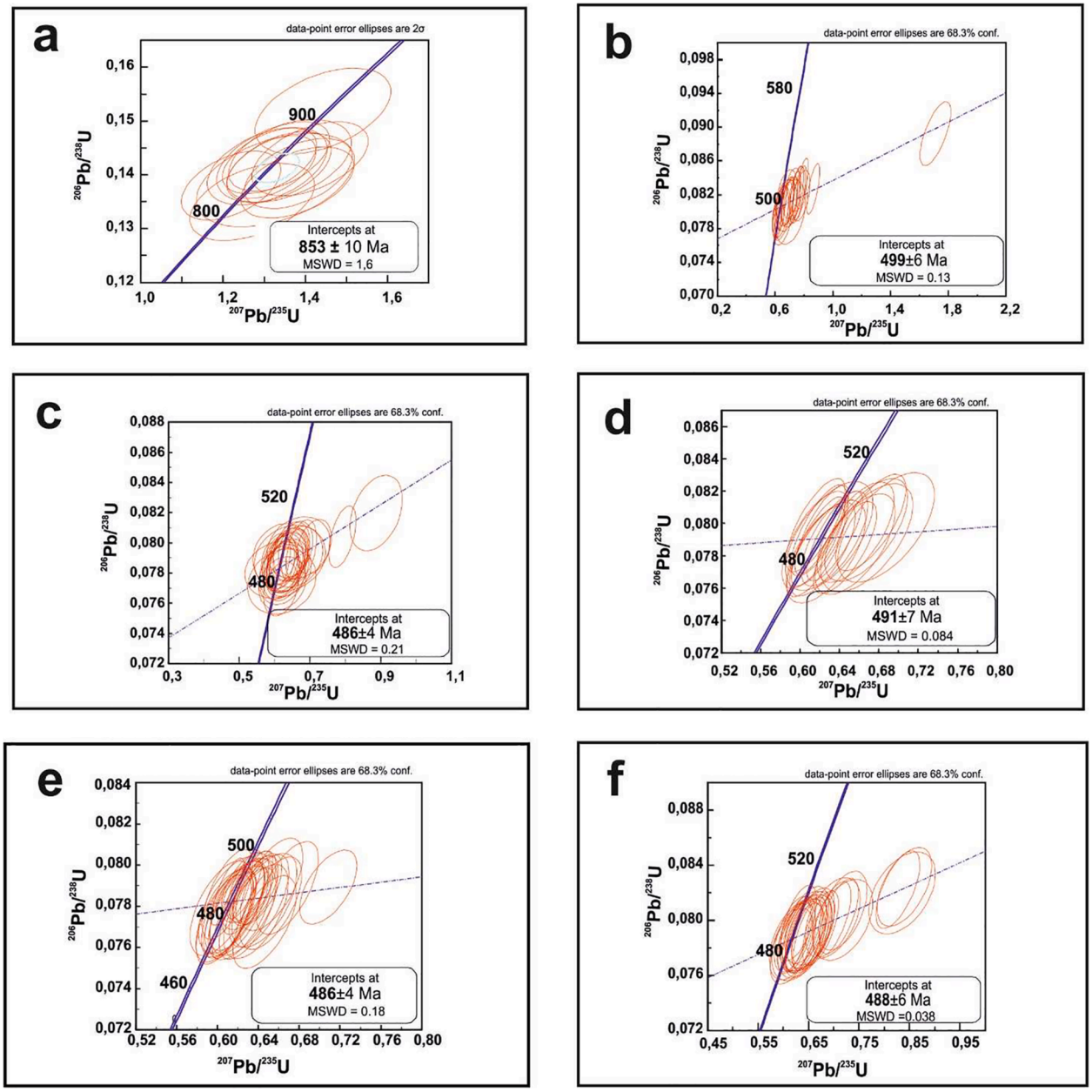

Fig. 5. Results of U-Pb dating of hosting granitoids. a – Tainskoye deposit (granodiorite); b – Sagangolskoye prospect (granodiorite); c – Konevinskoye deposit (granodiorite); d –Tumannoye prospect (leucogranites); e –Tumannoye prospect (granodiorites); f – Pogranichnoye prospect (granite).

Ore bodies of the Konevinskoe deposit are quartz lodes with quartz-sericite alteration halos (Fig. 13b). The main ore minerals are pyrite, tetradymite, chalcopyrite, galena, sphalerite, molybdenite, and native gold. There are also Sb-Bi-bearing sulfosalts (tetrahedrite, aikinite) and rare single grains of telluride minerals (petzite, hessite, coloradoite). Four mineral associations have been identified: 1) quartz-pyrite-molybdenite; 2) quartz-gold-pyrite; 3) gold-polysulfide; 4) Hg-bearing telluride. Two generations of native gold are distinguished. Gold-1 is included in the gold-quartz-pyrite association and characterized by fineness grades of 856-976‰ with the maximum of 925 – 950‰ (Fig. 13c. Gold-2 (fineness 719 – 943‰ and maximum 825 – 850‰) contains Hg impurities (up to 6.51 wt%). This gold prevails in ores and forms intergrowths with tetradymite, sometimes with galena and fahlore (Fig. 13d). Rare native gold-2 is present in quartz as isometric segregations. Au-Ag-Hg system minerals forming small inclusions in fahlore are widespread in the western part of the deposit. Geochemical specialization of the Konevinskoye ores can be presented as Au-Ag-Cu-Pb-Zn-Sb-Mo-Bi-Te-Hg with irregular component distribution.

The fluid inclusion study from quartz veins containing the gold-base metal sulfide association with tellurides (Damdinov et al., 2016) show that homogenization temperatures (T_h) of studied inclusions vary between 161 and 309 °C with an average value of 270 °C. There is a trend that FIs from central parts of the grains have higher T_h. Eutectic temperatures (-21 through –22°C) correspond to the salt system NaCl-H_2O. However, in some FIs, lower eutectic temperatures (−35 to −37 °C) indicate the presence of Fe and Mg chloride in the fluid composition. The bulk salinity is 8.7 – 12.9% eq. NaCl.

The sulfur isotope compositions were determined for pyrite, molybdenite, chalcopyrite, tetrahedrite, and sphalerite. The $\delta^{34}S$ values in all studied sulfide minerals have a narrow interval from −2.8 to +1.3‰ (see Table 1). The formation temperature calculated from sphalerite-pyrite pair is 274 °C (see Table 1, Sample Ko-14), which corresponds to the average value of the homogenization temperature. The sulfur isotopic composition of H_2S in the fluids in equilibrium with

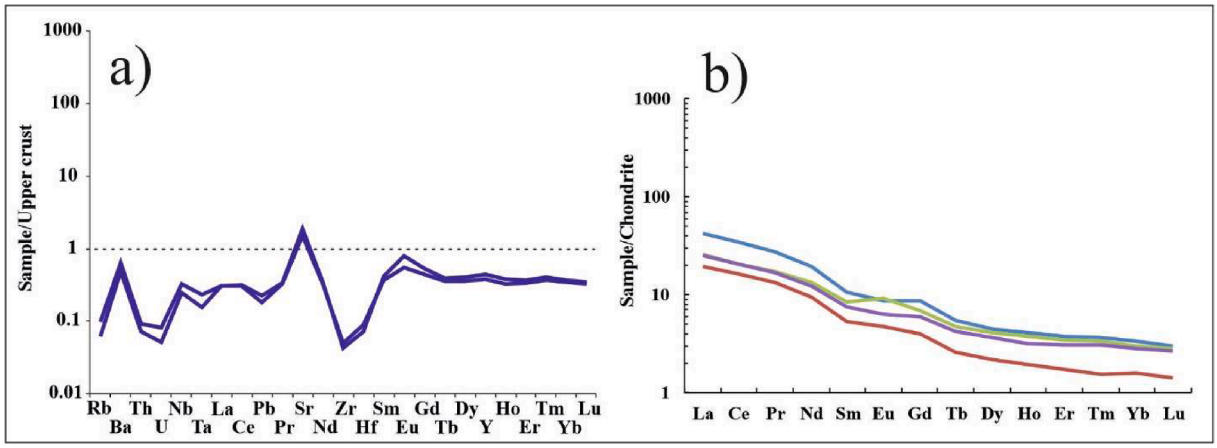

Fig. 6. Upper crust-normalized trace element (a) and chondrite-normalized REE (b) patterns for hosting granitoids from the Tainskoye deposit. Hereinafter the upper crust and chondrite values are according to (Rudnick and Gao, 2003) and (Sun and McDonough, 1989), respectively.

all studied sulfide minerals, based on obtained temperature T = 274 °C, ranges from −4.1 to −2.4‰. The oxygen isotopic compositions ($\delta^{18}O$) of ore-bearing quartz are 13.3 to 14.0‰. The calculation of the isotopic composition of the ore-forming fluid oxygen shows the values of 5.4 – 6.1‰ at 274 °C.

4.3. *Gold-stibnite mineralization*

Prospects containing gold-stibnite mineralization are known in the northwestern part of the studied region, within the Zhombolok gold cluster of the Khamsara metallogenic zone. The Tumannoye prospect is the largest, occurring as a series of quartz lode-streak zones in the granitoids of the Tannuol complex. Mineralization within the prospect contains stibnite (as the main mineral), pyrite, arsenopyrite, various Sb-bearing sulfosalts associated with native gold, and minor base metal sulfides.

4.3.1. ***Tumannoye prospect*** *(Fig. 2, No.4)*

Gold mineralization in the Tumannoye prospect is hosted in a leucogranite-granodiorite pluton (Damdinov et al., 2020a). The granitoids cut through gneisses and amphibolites of the Paleoproterozoic Bilinskaya suite, marbled limestones of the Early Paleozoic Bokson series, and Early Paleozoic subvolcanic rocks (Fig. 14).

Granitoids hosting the Tumannoe prospect (as well as Konevinskoe deposit (Saylag pluton)) belong to the Tannuol intrusive series. They are represented by dark-grey biotite-hornblende granodiorites and hydrothermally altered light-grey muscovite leucogranites, with SiO_2 contents of 62.9 – 64.1 wt% and 74.7 – 76.4 wt%, respectively. The leucogranites have K/Na ratios of 1.07 – 3.0, whereas the granodiorites have K/Na ratios of 0.61 – 0.66. Trace element patterns of these rocks are similar to those of the upper crust (Fig. 15a). REE distribution is similar for the two types of the granitoids. All rocks have some LREE enrichment (La/Yb_n = 5.6–15.2) but leucogranites have negative Eu anomalies (Eu/Eu*=0.47 – 0.58) (Fig. 15b). Generally, the geochemical features of the Tumannoye prospect granitoids are similar to the Saylag pluton. Therefore, we conclude that the Tannuol series granitoids might have been formed in the continental arc geodynamic setting.

Two spatially separated mineralized zones at the Tumannoye prospect are characterized by different mineral associations. Quartz lodes in slightly altered leucogranites contain a pyrite-arsenopyrite association with bismuth minerals (gold-bismuth association), whereas quartz-stibnite lodes (gold-antimony association) occur in cataclastic zones within gray medium-grained biotite-amphibole granodiorites. Most of these minerals are available in both types, and concentrations of most gold-related elements (Au, As, Bi, Te) in lodes of different types are similar, only Sb grades differ. In the gold-bismuth association, Sb content is up to 300 ppm, whereas in the gold-antimony association Sb content can reach 17.7 wt%. The main ore minerals are pyrite, arsenopyrite, and stibnite; minor, chalcopyrite, pyrrhotite, galena, sphalerite, molybdenite, andorite ($PbAgSb_3S_6$), kobellite ($Pb_{22}Cu_4(Bi,Sb)_{30}S_{69}$), zinkenite ($Pb_9Sb_{22}S_{42}$), argentian tetrahedrite, chalcostibite ($CuSbS_2$), aurostibite ($AuSb_2$), native bismuth, native antimony, and native gold. The gold fineness is 582 – 999‰. Three types of native gold are distinguished: low-fineness (582-725‰), medium-fineness (750-850‰) and high-fineness (850-999‰). These types of native gold correspond to three mineralization stages: gold-pyrite-arsenopyrite, gold-bismuth, and gold-antimony, respectively (Fig. 16a-c).

The fluid inclusions have a two-phase (gas–liquid) composition and a small size of 2–7 μm (Damdinov et al., 2020a). It was found that fluid inclusions from quartz containing a gold-bismuth association have homogenization temperature of 242 to 457 °C with an average of 295 °C. The interval for quartz containing gold-antimony association is 192 – 346 °C with an average value of 270 °C. The salinities of FI solutions from the quartz lodes with a gold-bismuth association (5.9 – 12.9% eq. NaCl) are generally higher than those in the quartz of a gold-antimony association (5.7 – 6.5% eq. NaCl). Eutectic temperatures are somewhat increased from earlier gold-bismuth −39 to −35 °C) to later gold-antimony associations (−35 to –32 °C). This indicates that the main dissolved salts change from Mg and Fe chlorides to Mg and Na chlorides from early to late mineralization stages. Mineral thermobarometry of the quartz-muscovite pair from the gold-bearing vein yields a temperature of 305 °C and the average pressure of 1847 bar whereas arsenopyrite thermometry shows a temperature of 280 °C (Damdinov et al., 2020a).

The sulfur isotope composition of stibnite from quartz-stibnite lodes has values from −1.9 to −3.8‰, whereas that of pyrite is 1.9‰ (see Table 1). The calculation of the sulfur isotopic composition of H_2S in the ore-forming fluid was conducted using temperature of 305 °C for pyrite and 280 °C for stibnite. Calculations yield $\delta^{34}S$ values of −1.5 to 0.7‰. The $\delta^{18}O$ values vary from 13.0‰ in quartz associated with pyrite-arsenopyrite (gold-bismuth association), to 15.8‰ in quartz of quartz-stibnite lodes with the gold-antimony association. The calculation of the isotopic composition of oxygen in the equilibrated fluids at 305 °C shows the $\delta^{18}O$ values ranging from 5.6‰ for the lodes, containing gold-bismuth association, to 8.4‰ for the lodes with the gold-antimony association.

Different types of granitoids hosting the Tumannoe prospect have similar zircon U-Pb ages: leucogranites hosting the lodes with the pyrite-arsenopyrite mineralization are dated as **491 ± 7** Ma (Fig. 5d); granodiorites hosting the quartz-stibnite lodes have an age of **486 ± 4** Ma (Fig. 5e). Thus, granitoids hosting mineralization on different sites, despite some differences in their mineral and chemical compositions, are

Table 1
S and O isotopic compositions of sulfides and quartz from the intrusion-hosted deposits of the South-East of Eastern Sayan.

Sample	$\delta^{34}S$ (‰)	$\delta^{34}S_{fl}$	$\delta^{18}O$ (‰)	$\delta^{18}O_{fl}$	Mineral	Deposit	Type of the deposit
Tn-11	3.7	3.1			Pyrrhotite	Tainskoye (Mironov et al., 2001; this study)	Gold-telluride
Tn-11	3.2	3.1			Chalcopyrite		
Tn-213	4.1	3.1			Pyrite		
Tn-450	3.2	2.6			Pyrrhotite		
Tn-39	4.3	3.7			Pyrrhotite		
Tn-39	4.5	4.4			Chalcopyrite		
Tn-448	3.6	3.0			Pyrrhotite		
Tn-458	3.1	3.0			Chalcopyrite		
Gg-48			13.2	8	Vein quartz		
Tn-450			13.3	8.1	Vein quartz		
Bs-3	−3.2	−4.4			Pyrite	Sagangolskoye (Damdinov et al., 2007; this study)	
Bs-35	1.2	0.0			Pyrite		
Bs-80	−2.9	−4.1			Pyrite		
K-4238	−4.2	−5.4			Pyrite		
Bs-116			8.9		Quartz from granites		
Bs-136			12.7	5.8	Vein quartz		
Bs-58			13.3	6.4	Vein quartz		
Hr-80	−2.1	−3.3			Pyrite	Khoringolskoye (Damdinov et al., 2007; this study)	
Hr-29	1.1	−0.1			Pyrite		
Hr-136	4.3	3.1			Pyrite		
Hr-513	1.3	0.1			Pyrite		
Hr-518	0.0	−1.2			Pyrite		
Hr-519	0.2	−1.0			Pyrite		
Hr-520	0.7	−0.5			Pyrite		
Hr-136			8.9	2.0	Vein quartz		
Hr-513			10.8	3.9	Vein quartz		
Hr-518			10.9	4.0	Vein quartz		
Hr-520			11.3	4.4	Vein quartz		
Tu-27	−3.5	−1.2			Stibnite	Tumannoye (Damdinov et al., 2020a; this study)	Gold-stibnite
Tu-30	−2.5	−0.2			Stibnite		
Tu-44	−3.8	−1.5			Stibnite		
1962-1	−1.9	0.4			Stibnite		
Tu-20	1.9	0.7			Pyrite		
Tu-13			13.0	6.0	Vein quartz		
Tu-20			13.1	6.1	Vein quartz		
Tu-9к			14.2	7.2	Vein quartz		
Tu-9c			8.7	7.2	Muscovite		
Tu-50			15.1	8.2	Quartz from quartz-stibnite veins		
Tu-30			15.8	8.9	Quartz from quartz-stibnite veins		
Tu-23			12.5		Quartz from granites		
Tu-4			9.6		Quartz from granites		
Tu-41			11.3		Quartz from granites		
Ko-14	−1.2	−2.5			Pyrite	Konevinskoye (Damdinov et al., 2016; present study)	Gold-tetradymite
Ko-14	−2.2	−2.5			Sphalerite		
Ko-1-1	0.2				Molybdenite		
Ko-5	1.3				Molybdenite		
Ko-22	0.7				Molybdenite		
Ko-4	−2.2	−2.4			Chalcopyrite		
Ko-13	−2.6	−3.9			Pyrite		
Ko-14-1	−2.8	−4.1			Pyrite		
Ko-39	−2.6	−3.9			Pyrite		
181.8			13.3	5.4	Vein quartz		
48M			14.0	6.1	Vein quartz		
Ko-26			9.9		Quartz from granites		
Pg-19	7.6	6.4			Pyrite	Pogranichnoye (Garmaev et al., 2013; present study)	Gold-Bi-sulfosalt
Pg-25	6.9				Arsenopyrite		
Pg-79	6.8				Arsenopyrite		
Pg-338	7.4	6.2			Pyrite		
Pg-435	4.9				Arsenopyrite		
Pg-17			11.3		Quartz from granites		
Pg-78			12.1		Quartz from greisen		
Pg-318			12.9	6.4	Vein quartz		
Pg-575			14.0	7.5	Vein quartz		
Pg-380			14.1	7.6	Vein quartz		
Pg-562			14.3	7.8	Vein quartz		

Note: fl – equilibrium fluid. Temperatures of equilibrium fluid isotopic compositions calculations are presented in the text, using functions of Ohmoto and Rye (1979) and Sharp et al. (2016).

similar in age and refer to different phases of one (Tannuol) intrusive series. The mineralization age, determined by $^{40}Ar/^{39}Ar$ dating of muscovite from a gold mineralized quartz lode, is **439.4 ± 3.5** Ma (Fig. 8b).

4.4. Gold-bismuth-sulfosalt mineralization

Mineralization with the gold-bismuth-sulfosalt assemblage is associated with orogenic leucogranites of the Early Paleozoic Sarkhoy intrusive series, and is represented by the Pogranichnoye prospect. The

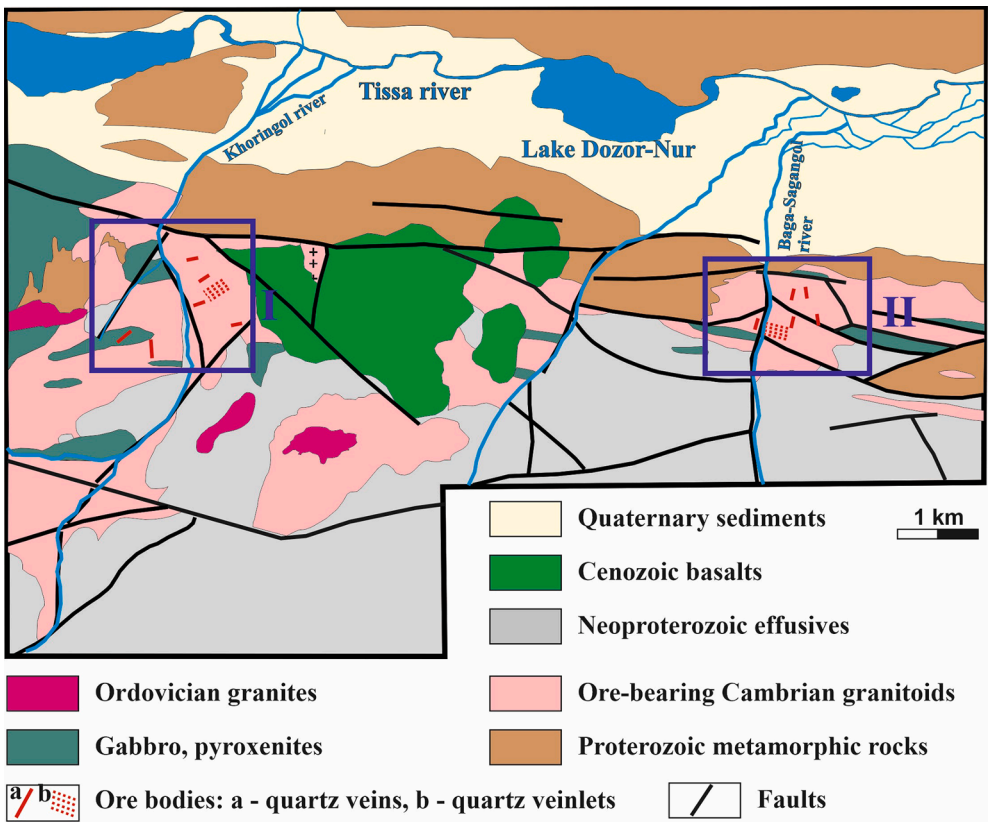

Fig. 7. Geological map of the Tissa-Sarkhoi gold cluster showing the Khoringolskoye (I) and Sagangolskoye (II) gold prospects (after V. F. Stavsky's unpublished materials).

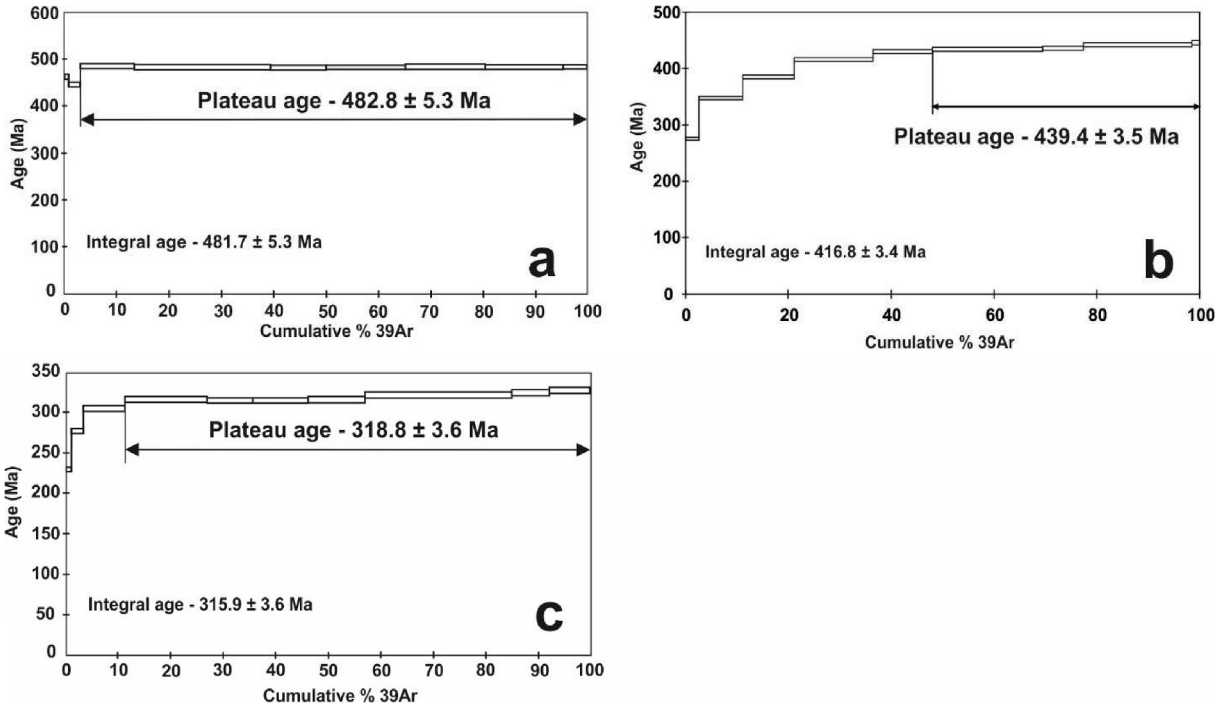

Fig. 8. Results of 40Ar/39Ar dating: a – sericite from the Khoringolskoye prospect's quartz-sericite rocks; b – muscovite from a mineralized quartz vein at the Tumannoye prospect; c – muscovite from the Pogranichnoye prospect greisen.

main gold-related minerals are pyrite and arsenopyrite with minor base metal sulfides and sulfosalts. However, the bulk of the native gold is associated with Bi-bearing minerals, such as bismuthine, galenobismuthite, lillianite, and native bismuth. The prospect is characterized by the features of geological structure and ore composition corresponding to intrusion-related deposits of the gold-bismuth type in the

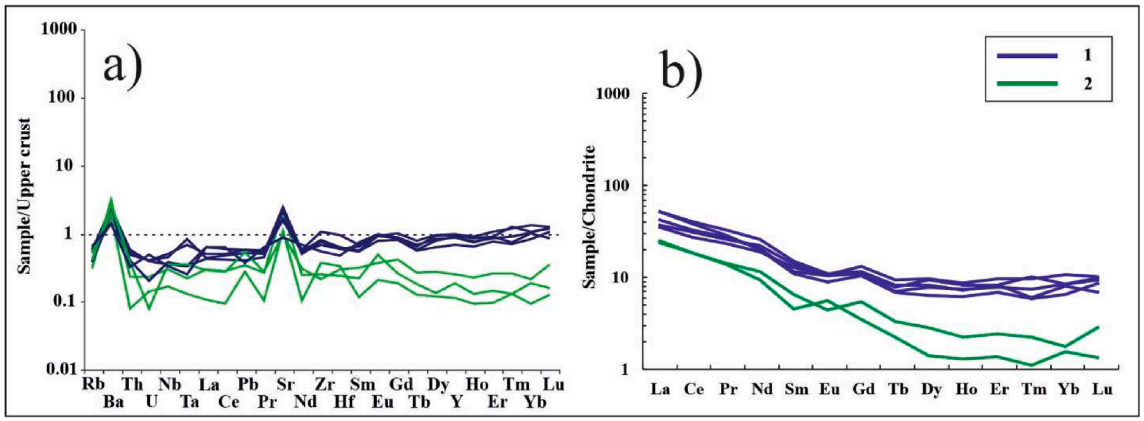

Fig. 9. Upper-crust normalized trace element (a) and chondrite-normalized REE (b) patterns for hosting granitoids of the Khoringolskoye and Sagangolskoye prospects.

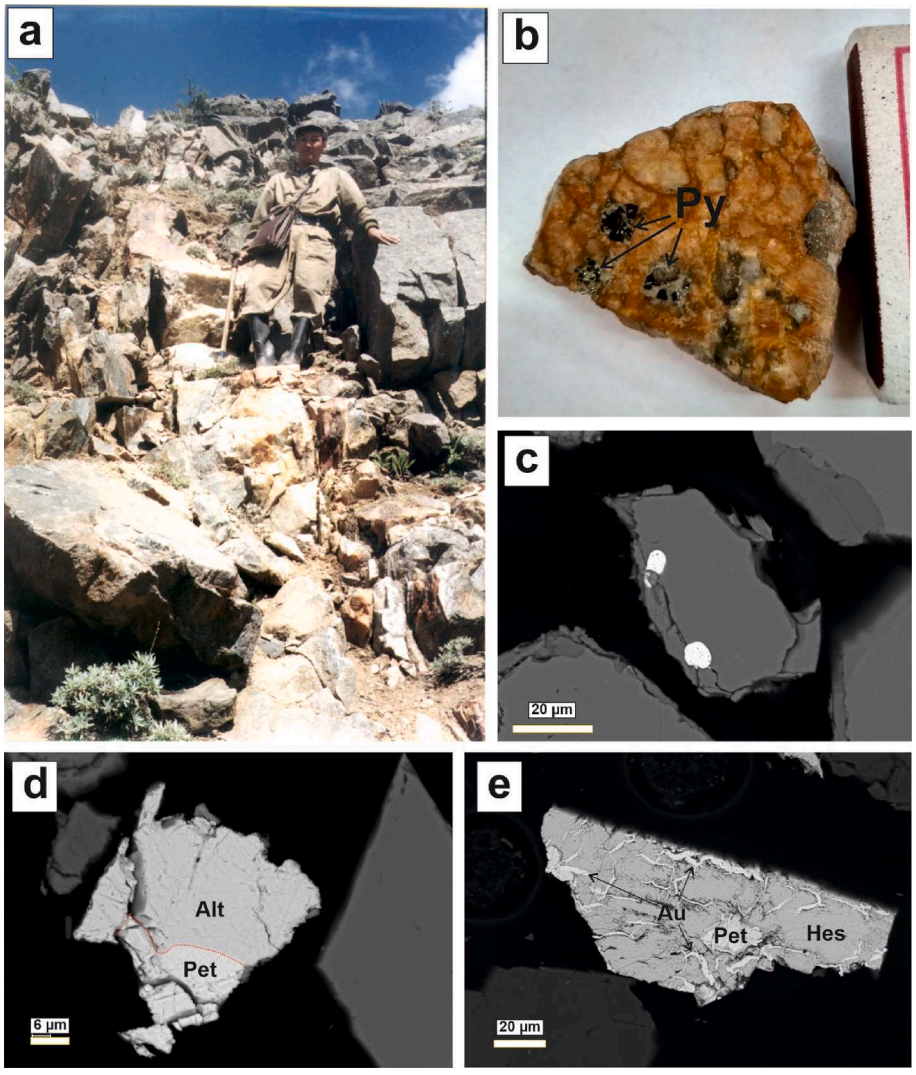

Fig. 10. Vein and mineralization morphology in the gold prospects of the Tissa-Sarkhoi gold cluster: a - field photographs of a quartz vein in the Khoringolskoye prospect; b - clumpy sulfides in coarse-grained plagiogranite from the Sagangolskoye prospect; c – native gold inclusions in pyrite; d – association of petzite (Ag_3AuTe_2) with altaite (PbTe) (Khoringolskoye prospect); d – hessite ($AgTe_2$)-native gold association with petzite relic (Sagangolskoye prospect). Mineral abbreviations: Py – pyrite, Alt – altaite, Pet - petzite, Au – native gold, Hes – hessite.

North-East of Russia (Goryachev and Gamyanin, 2006; Vikent'eva et al., 2018). Moreover, accessory minerals, such as scheelite, molybdenite as well as native gold, silver, arsenopyrite, pyrite, native bismuth, identified in the mineralized granites, are also present in the gold-bearing veins, although the gold content in the mineralization zones is low.

4.4.1. *Pogranichnoye prospect (Fig. 2, No. 5)*

Gold mineralization of the prospect is hosted in the leucogranite massif that cuts through Neoproterozoic volcanogenic-sedimentary deposits of the Dibinskaya suite, metamorphosed volcanic rocks of the Sarkhoy series and Early Paleozoic carbonate rocks of the Bokson series (Fig. 17; Damdinov et al., 2009; Garmaev et al., 2013).

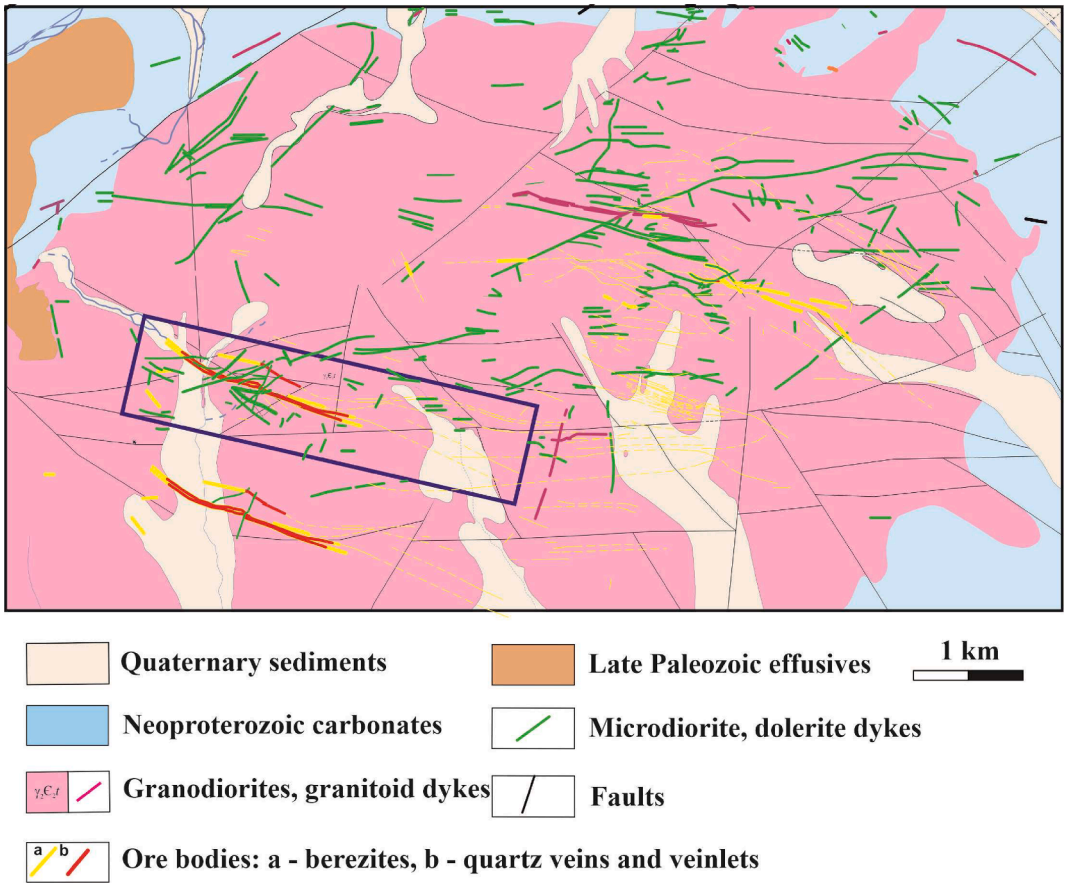

Fig. 11. Geological map of the Saylag pluton showing the Konevinskoye gold deposit setting (blue rectangle; based on P. A. Roschektayev's unpublished materials). (For interpretation of the references to colour in this figure legend, the reader is referred to the web version of this article.)

Table 2
Molybdenite Re-Os dating results from the Konevinskoye gold deposit.

Sample	Common Os(ng/g)	Common Os(ng/g)	^{187}Re	^{187}Re	^{187}Os	^{187}Os	Re (ng/g)	Re (ng/g)	Model age	Model age
		1σ		1σ		1σ		1σ		1σ
Ko-22	0.171	0.009	19,661	853	150.74	1.22	31,408	1363	458.5	3.7

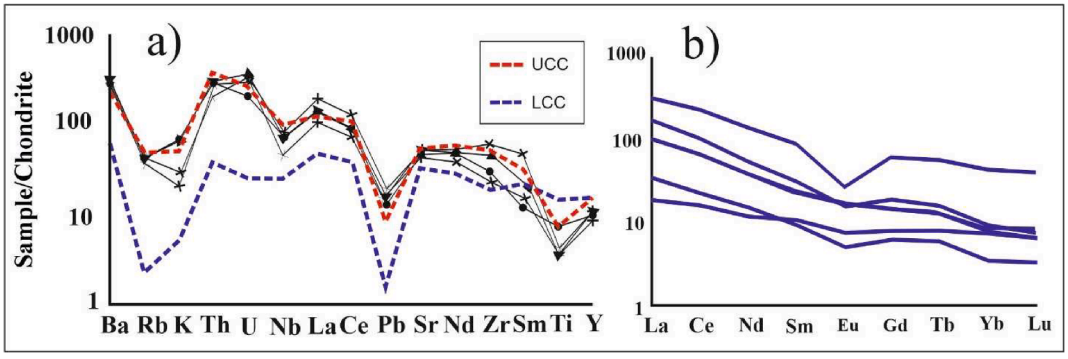

Fig. 12. Chondrite-normalized trace element (a) and REE (b) patterns for hosting granitoids from the Konevinskoye deposit. UCC – upper continental crust, LCC – lower continental crust (Rudnick and Gao, 2003).

Granitoids hosting the mineralization are represented by medium-grained biotite and hornblend-biotite granites. The granitoids have relatively high SiO_2 contents of 75.6 to 78.4 wt% and K/Na ratios of 1.11 – 2.31 with the average of 1.4. These rocks have comparable with an upper crust LILE and HFSE contents. However, upper crust normalized spider diagrams have negative Ba, Sr, Eu and positive Th, U, Pb anomalies (Fig. 18a). The REE distribution curves have LREE enrichment and negative Eu anomalies (La/Yb_n = 8.9 – 11.8) (Fig. 18b). The geochemical characteristics of the studied granitoids correspond to orogenic granites (Garmaev et al., 2013).

Slightly altered granites have increased contents of ore-forming elements (As, Sb, Cu, Zn, Pb, and Mo). Accessory minerals in the unaltered

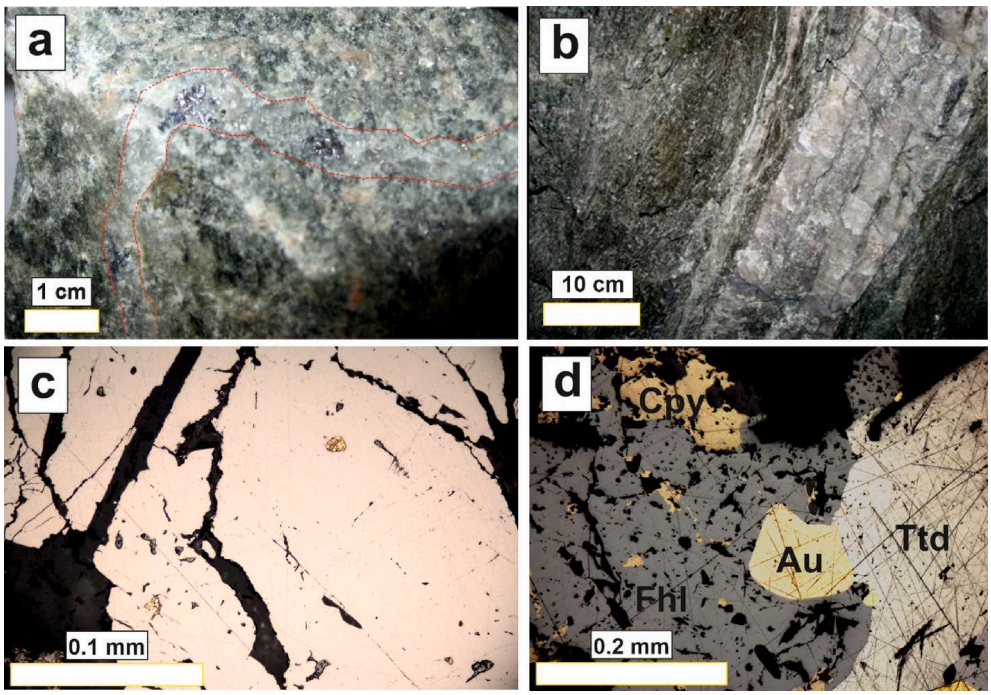

Fig. 13. Vein and mineralization morphology in the Konevinskoye deposit: a – quartz-molybdenite veinlet in the granodiorite; b – quartz vein with a quartz-sericite altered granitoid rim; c – native gold inclusions in pyrite; d – native gold associated with tetradymite, fahlore (tetrahedrite), and chalcopyrite. Mineral abbreviations: Mol – molybdenite, Au – native gold, Ttd – tetradymite, Fhl - fahlore, Cpy – chalcopyrite.

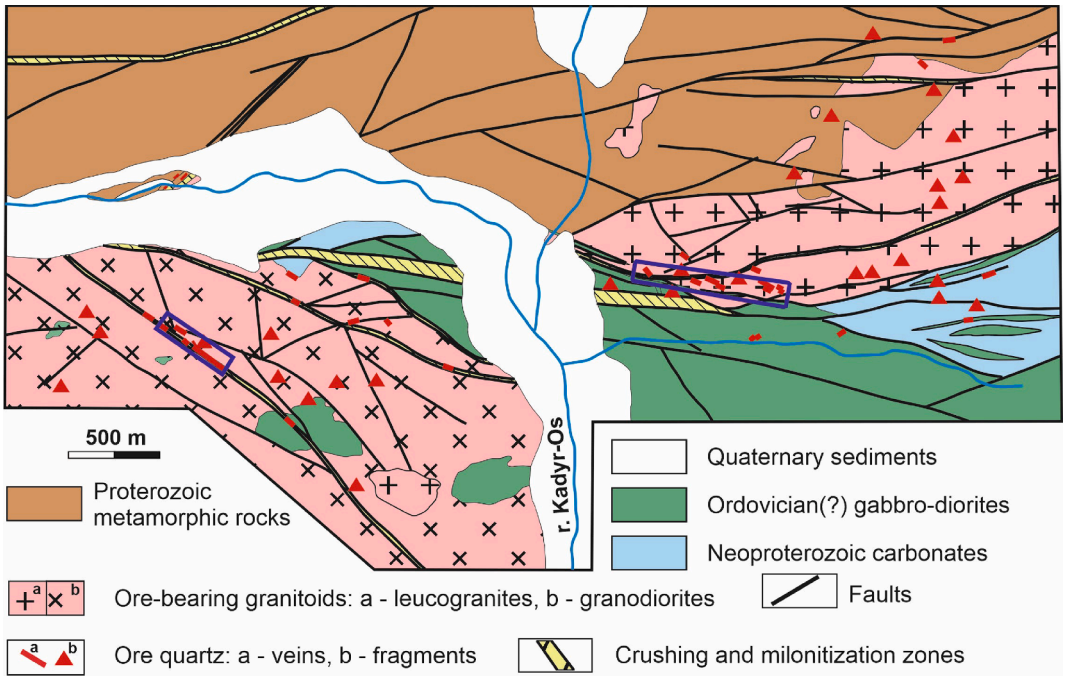

Fig. 14. Geological map of the Tumannoye gold prospect (based on V. S. Grachyov's unpublished materials).

granites include molybdenite, native gold, silver as well as tellurides of Au, Ag, Pb. Mineralization zones are represented by quartz lodes and streaks rimmed with greisen zones. Three ore mineral associations can be identified as pyrite-arsenopyrite, sphalerite-galena (base metal-sulfide), and gold-bismuth-sulfosalt. The specific gold-bismuth-sulfosalt association is rather widespread but quite dispersed. Sulfosalts are represented by tetrahedrite, boulangerite, jamesonite associated with bismuth-bearing minerals, such as bismuthine, galenobismuthite, lillianite, as well as native bismuth (Fig. 19a) and native gold. Gold grains in pyrite are 10–20 μm (Fig. 19b). Gold fineness varies from 710 to 988‰. But most of the fineness values fall within the range between 850 and 925 ‰. The Pogranichnoye prospect gold mineralization contains a specific geochemical association of As-Bi-Pb-Sb-Cu-Au that differs from the other gold deposits in the studied region. Gold concentrations are not high, varying between 0.15 and 1.3 ppm.

The arsenopyrite formation temperatures, calculated using an

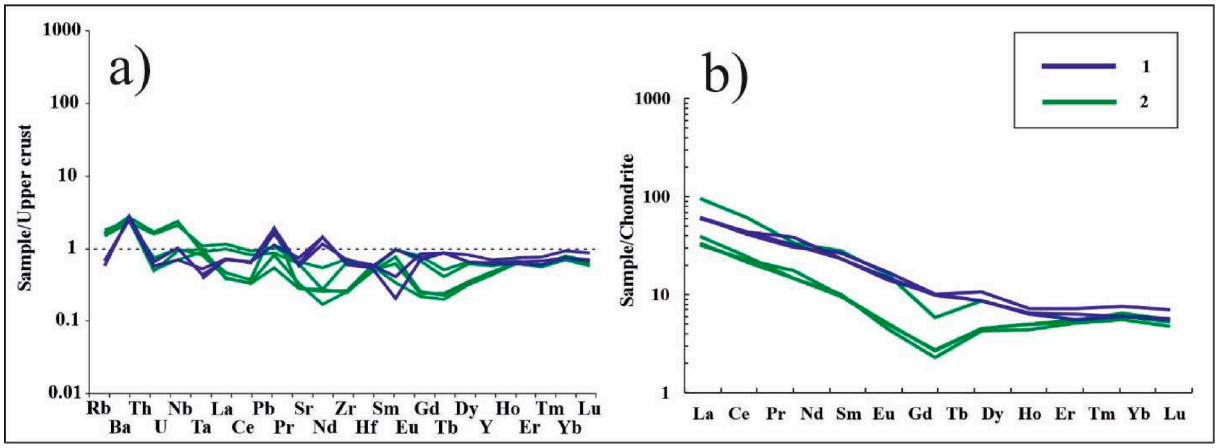

Fig. 15. Upper crust-normalized trace element (a) and chondrite-normalized REE (b) patterns for hosting granitoids from the Tumannoye prospect.

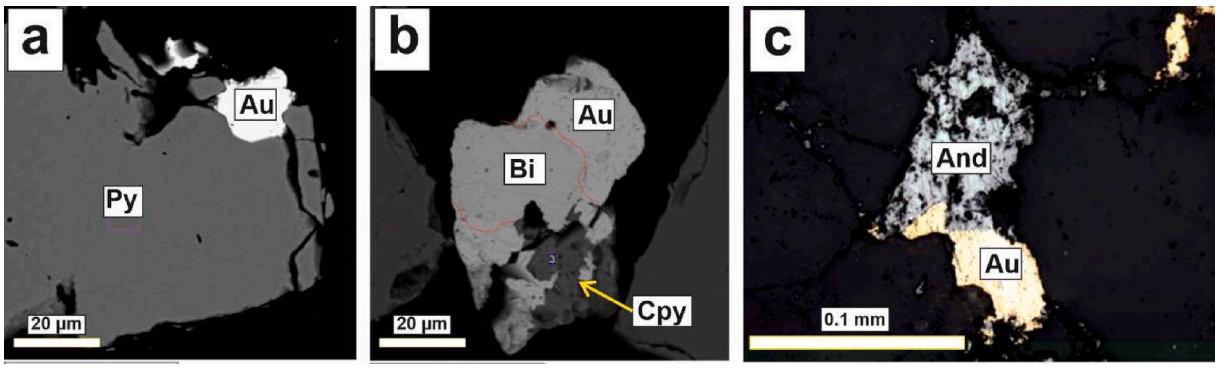

Fig. 16. Gold-related minerals in the Tumannoye gold prospect: a – native gold grain (Au) in pyrite (Py); b – association of native gold (Au) and bismuth (Bi) corroded chalcopyrite (Cpy); c – association of native gold (Au) with andorite (And) ($AgPbSb_3S_6$).

arsenopyrite geothermometer (Kretschmar and Scott, 1976), show a range from 300 to 507 °C. The modal interval of the temperature values is 400 – 450 °C, with an average value of 419 °C. Arsenopyrite formed before Bi-bearing sulphosalts. The same relatively high-temperature conditions of the Bi-sulphosalt association were identified in the Larga hydrothermal system in Romania (Cook and Ciobanu, 2004) and in the Sredne-Golgotay gold-bismuth deposit in eastern Transbaikalia (Gvozdev et al., 2020). Nevertheless, the existence of native bismuth testifies to the temperature not exceeding 271 °C. It can be assumed that the temperature decreased from over 400 °C to under 270 °C from pyrite-arsenopyrite to bismuth-sulphosalt associations.

The fluid inclusion study was carried out using 15 primary fluid inclusions only. The studied inclusions are extremely small in size (≤5 – 8 μm) and have a two-phase (liquid > gas) composition. Groups of cogenetic, fluid-dominated, and vapour-dominated inclusions within one growth zone were observed in some grains, which indicates fluid heterogenization (boiling). This implies homogenization temperatures corresponding to the inclusion trapping (host mineral formation) temperatures. Measured homogenization temperatures vary from 275 to 380 °C with an average of 313 °C. The bulk salinity of solutions is relatively low, varying from 3.1 to 9.6% eq. NaCl. The eutectic temperature interval (–33.5 to −38 °C) shows Fe and Mg chlorides dominate in the salt composition of the fluids.

Pyrite and arsenopyrite have $\delta^{34}S$ values of 4.9 – 7.6‰, where pyrite is characterized by ^{34}S enrichment in comparison with arsenopyrite (see Table 1). The $\delta^{34}S$ values of equilibrium fluids for temperature of 313 °C are 6.2 – 6.4‰. Oxygen isotopic composition in the lode quartz varies from 12.9 to 14.0‰. The $\delta^{18}O$ values calculated for the equilibrium fluids at a temperature of 313 °C range from 6.4‰ to 7.8‰.

U-Pb dating of zircon from leucogranites hosting the Pogranichnoe prospect yields an age of **488 ± 6** Ma (Fig. 5f). $^{40}Ar/^{39}Ar$ dating of muscovite from the quartz lode yields a younger isotopic age of **318.8 ± 3.6** Ma (Fig. 8c). Our previously obtained K-Ar date for muscovite from host greisen gives the age of **537 ± 11** Ma. As well as in the case of the Sagangolskoye prospect, this K-Ar date may reflect the Early Paleozoic age of mineralization.

5. Discussion

5.1. The age of gold mineralization

The earliest papers on gold deposits in the area under discussion were published in the 1960s. Most of the gold deposits were presumed to be related to granitoid plutons (Feofilaktov, 1970). Both the granitoids and gold deposits were considered to be of Early Paleozoic age. Later it was established that the largest orogenic deposits of this region were much younger than spatially associated granitoids (Damdinov et al., 2018; Mironov and Zhmodik, 1999; Goldfarb et al., 2001, 2014). Nevertheless, rare intrusion-related deposits were identified in the region (Garmaev et al., 2013; Damdinov et al., 2007; 2009, 2016; Mironov et al., 2001). However, the absence of isotopic age data on these deposits and ore-hosting granitoids prevented from verification of an association. Earlier, some granitoids had been dated using Rb-Sr and K-Ar methods, but the data obtained were equivocal due to the secondary alteration of granitoids. Nevertheless, some of those results were used in this study (Table 3).

The oldest island arc granitoids of the Tainsky pluton formed at 853 ± 10 Ma (Damdinov et al., 2020b). Rhenium-osmium dating of

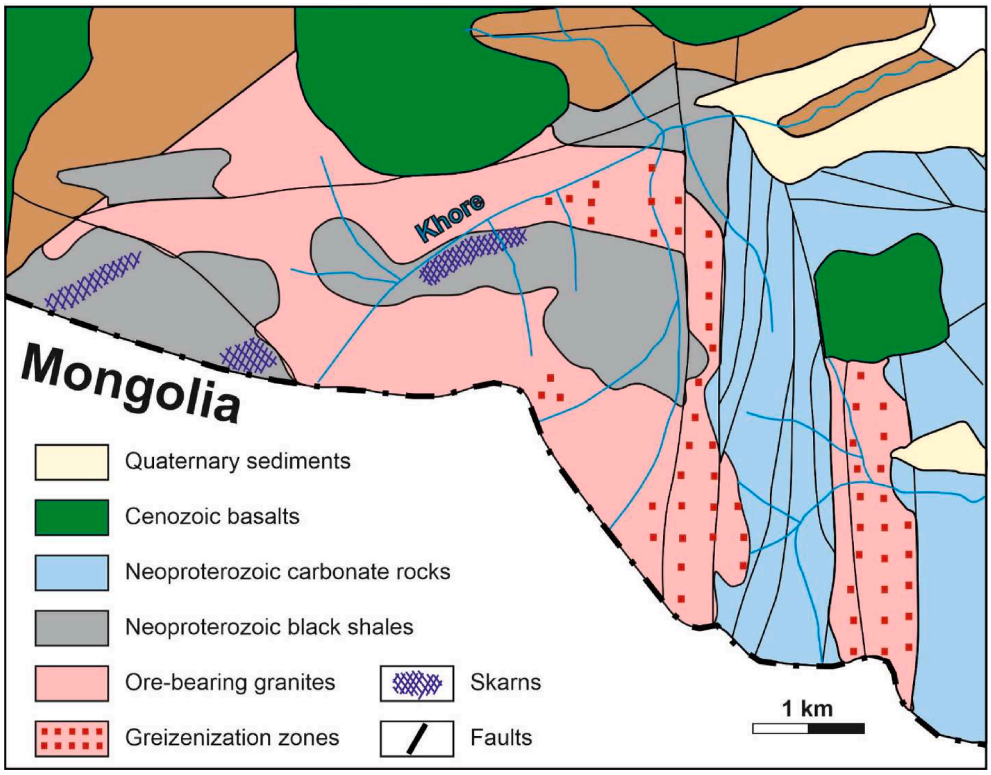

Fig. 17. Geological map of the Pogranichnoye gold prospect (based on Dibinskaya's geological party materials).

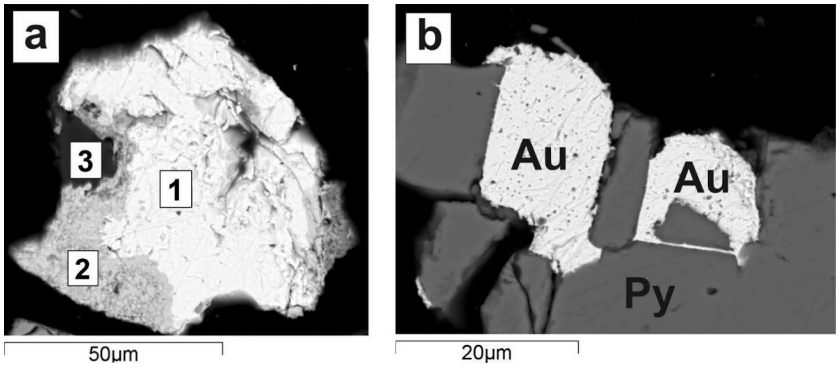

Fig. 18. Upper crust normalized trace element (a) and chondrite normalized REE (b) distribution diagrams for hosting granitoids in the Pogranichnoye prospect.

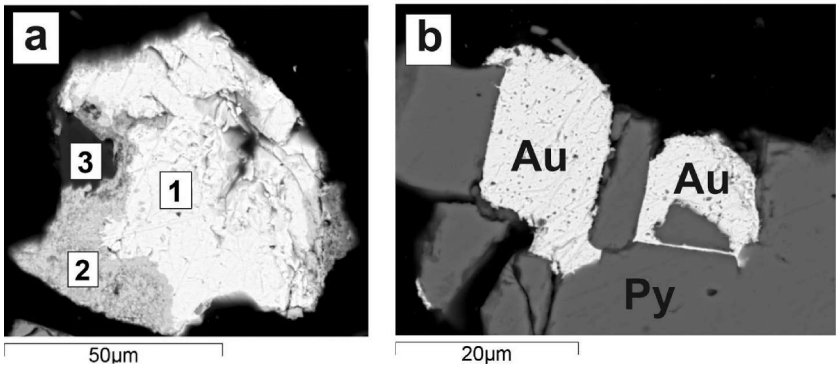

Fig. 19. Mineralization in the Pogranichnoye prospect: a – lillianite ($Pb_3Bi_2S_6$) (1) with quartz (3) and Bi arsenate (2); b – native gold (Au) grains in pyrite (Py).

Table 3
Isotope dating results for the studied gold deposits and prospects.

Deposit (prospect)	Age, Ma	Dating system	Mineral	Notes	Source
Tainskoye deposit	853 ± 10	U-Pb	Zircon		Damdinov et al., 2020b
	855.8 ± 5.1	Ar/Ar	Hornblende		
	860	Re-Os	Molybdenite		Mironov et al., 2005
Konevinskoye deposit	486 ± 4	U-Pb	Zircon		This study
	458.5 ± 3.7	Re-Os	Molybdenite		This study
	324 ± 5.3	Ar/Ar	Biotite	Late dykes	Damdinov et al., 2016
Sagangolskoye prospect	499 ± 6	U-Pb	Zircon		This study
	482.3 ± 5.3	Ar/Ar	Muscovite		This study
	537 ± 15	Rb-Sr	Bulk rock	Near-lode quartz-sericite altered rocks	Damdinov et al., 2007
Pogranichnoye prospect	488 ± 6	U-Pb	Zircon		This study
	318.8 ± 3.6	Ar/Ar	Muscovite		This study
	537 ± 11	K/Ar	Muscovite		This study
Tumannoye prospect	491 ± 7	U-Pb	Zircon	Leucogranite	Damdinov et al., 2020a
	486 ± 4	U-Pb	Zircon	Granodiorite	
	439.4 ± 3.5	Ar/Ar	Muscovite		

molybdenite from the Tainskoe deposit ore shows a similar age of 860 Ma (Mironov et al., 2005). Unfortunately, the cited paper has no reference to the analytical error. Nevertheless, considering the analytical error of U-Pb dating, these data indicate synchronous granitoids formation and ore mineralization. This permits the identification of a Neoproterozoic stage of intrusion-hosted gold deposit formation in the studied region. However, the fact that the Tainskoye deposit and the Tainsky granitoid stock are the only example identified, raises the possibility that the bulk of the Neoproterozoic island arc granitoids may have been subsequently eroded.

Similar island arc granitoids host the Khoringolskoe and Sagangolskoe gold prospects. But the age of these granites is Early Paleozoic (499 ± 6 Ma). The Early Paleozoic age of 537 ± 15 Ma was obtained earlier by Rb-Sr dating of quartz-sericite rocks from diffusion rims (Damdinov et al., 2007). However, the $^{40}Ar/^{39}Ar$ age of near-lode quartz-sericite altered rocks is 482.8 ± 5.3 Ma. It is assumed that ore formation took place relatively later than parent granitoid crystallization. Nevertheless, the dating results confirm the Early Paleozoic age of the granites and the mineralization event.

Dating of the Tannuol series granitoids, hosting the Konevinskoye deposit and the Tumannoye prospect, shows their Early Paleozoic ages. In particular, granodiorites hosting the Konevinskoe deposit and quartz-stibnite veins of the Tumannoye prospect show the same age values of 486 ± 6 and 486 ± 4 Ma, respectively. Leucogranites hosting the gold-bismuth association in the Tumannoye prospect have the slightly earlier age of 491 ± 7 Ma. Re-Os molybdenite and $^{40}Ar/^{39}Ar$ muscovite ages of the ores are 458.5 ± 3.7 and 439.4 ± 3.5 Ma for the Konevinskoye deposit and the Tumannoye prospect, respectively. These ages are slightly younger than the results of U-Pb dating, but still indicate the Early Paleozoic age of the ore mineralization. A cause of this difference may be long cooling of the granite massif (Travin et al., 2020). The Late Paleozoic (324 ± 5.3 Ma) age of the dykes cutting the ore-hosting granitoids in the Konevinskoye deposit (Damdinov et al., 2016) reflects the later stage of ore-forming process where early gold-bearing assemblages transformed and were enriched with Hg and probably Te.

The age of the orogenic granites hosting the Pogranichnoye prospect is 488 ± 6 Ma. Dating of the mineralization using $^{40}Ar/^{39}Ar$ and K/Ar method yields controversial results. The Ar/Ar age of muscovite from a quartz vein is 318.8 ± 3.6 Ma, whereas the K/Ar age of muscovite from a diffusional near-lode greisen rim is 537 ± 11 Ma. It shows that the Ar isotope system was broken by post-ore tectonic processes. Nevertheless, the discussed Pogranichnoye prospect totally coincides with the intrusion-related gold-bismuth deposits from the north-east of Russia in ore mineralogy, geological setting, and isotope composition (Goryachev and Gamyanin, 2006; Goryachev and Pirajno, 2014; Vikent'eva et al., 2018). In addition, some ore minerals were found in accessory assemblages of the ore-hosting granites, which proves the relationships between the gold mineralization and hosting granites.

The obtained data on the age of the deposits and prospects under research show some dissimilarity of U-Pb, Re-Os and $^{40}Ar/^{39}Ar$ dates. According to data by Travin et al. (2020), crystallization of large granite plutons can occur over an extended period of from up to 100 and more million years. Therefore, $^{40}Ar/^{39}Ar$ dates are often younger than U-Pb ages (zircon). Conjugate dating of zircon and minerals with different $^{40}Ar/^{39}Ar$ isotope system closing temperatures allows tracing crystallization time of all minerals comprising the dated rock or rock assemblage. This property is the basis for the thermochronology method (Dodson, 1973; Hodges, 2004). Moreover, $^{40}Ar/^{39}Ar$ dates are susceptible to the influence of late tectonic events and may reflect the age of these events and be rejuvenated (Brown, 2009). We observed this rejuvenation in the hosting granitoids of the Tainskoye gold deposit where different values of isotopic ages, ranging from 855.8 ± 5.1 to 223.5 ± 1.6 Ma, were found reflecting different stages of the East Sayan tectonic evolution (Damdinov et al., 2020b). Furthermore, ore-bearing fluids be derived during the later stages of the host granites crystallization. Considering that the granite pluton crystallization can take a relatively long time, ore formation can occur later than magmatism. An age difference between intrusion and mineralization in excess of 15 m.y. was established at the gold deposits associated with orogenic granites in Russia's Far East (Goryachev and Pirajno, 2014).

Isotopic dating of gold mineralization allows differentiation of two main age stages of intrusion-hosted gold deposits in the studied region: Neoproterozoic (**850–860** Ma) and Early Paleozoic (**458–439** Ma), corresponding to the main orogenic stages of the region (Fedotova and Khain, 2002; Gordienko et. al., 2016; Kuzmichev, 2015).

The Neoproterozoic orogenic stage was initiated by the collision between the Dunzhugar island arc and the Gargan continental block. This process was accompanied by obduction of the Dunzhugur ophiolites over the Archean basement of the Gargan block, which resulted in the formation of the Tuva-Mongolian microcontinent. It is believed that the Dunzhugur island arc magmatism began before 1034–1022 Ma and ended between 850 and 800 Ma, according to the published ages of island arc granitoids (Khain et al., 2002; Kuzmichev 2015) and to our data (853 ± 10 Ma). At that time, probably at the final stage of island arc magmatism, the gold-telluride deposits were formed. Available geochronological data indicate the Dunzhugur island arc persisted within the Paleoasian Ocean over the extended period from 1034 to 800 Ma. Over this period of near 200 m.y., several island arcs may have been developed, but the paucity of geochronological data has inhibited interpretation of the late Meso- and Neoproterozoic history of the region.

After the accretion of the Dunzhugur island arc and the obduction of early ophiolites, at the margin of the Tuva-Mongolian microcontinent, the Sarkhoy volcanic arc formed (Kuzmichev et al., 2015). Rock assemblages of the Sarkhoy arc, represented by metamorphosed volcanic rocks of the Sarkhoy series (**782** Ma), are comagmatic with the

Neoproterozoic TTG-granitoids of the Sumsunur series (**790** Ma) (Kuzmichev, 2015). Geochemically, these rocks correspond to the continental arc granitoids. However, no gold mineralization was developed over the period between 850 and 500 Ma.

The main late orogenic stage began in the region at 500 Ma. During the period between 500 and 486 Ma a series of granitoids with different geochemical compositions were formed. Due to the complex tectonomagmatic evolution of East Sayan, these granite series were probably derived in different tectonic settings including island arc-, continental arc- and orogenic granites. The Early Paleozoic island arc-type granitoids, possibly producing the gold-telluride mineralization (Khoringolskoye and Sagangolskoye prospects) type, might have been formed within the Sarkhoy volcanic arc. Simultaneously, in the northwestern (in present-day coordinates) part of the southeastern East Sayan a continental arc existed with magmatism represented by granitoids of the Tannuol magmatic series, hosting gold-stibnite (Tumannoye prospect) and gold-tetradymite (Konevinskoye deposit) mineralization. Orogenic-type granites, hosting gold-bismuth-sulfosalt mineralization (Pogranichnoye prospect), were formed in the modern southern part of the region researched. However, Ar/Ar and Re-Os dating data present the relatively younger age of the gold mineralization: 458 – 439 Ma (Konevinskoye deposit and Tumannoye prospect, respectively). This age period is consistent with the middle of the late orogenic, post-subduction period (500 – 420 Ma, Damdinov et al., 2018).

The age data on the ore-hosting granitoids may indicate that in the Early Paleozoic (about 500–486 Ma) island arcs, continental arcs, and orogenic zones existed simultaneously in different parts of the modern East Sayan. Alternatively, granites with different geochemical features might have formed during the orogeny due to different substrates melting. Both hypotheses are consistent with the fact that the closure of the Paleo-Asian Ocean and formation of the northern part of the Central Asian Orogenic Belt took a relatively long time in the range of 500 – 420 Ma (Damdinov et al., 2018). These events resulted in the formation of large gold-quartz and gold-sulfide-quartz orogenic gold deposits (Zun-Kholba, Barun-Kholba, Pioneer deposits, etc.) as well as the emergence of gold deposits in association with granitoids of different origins.

The Late Paleozoic tectonic-magmatic activation is reflected in dyke magmatism and regional strike-slip deformations widely spread within the whole Central Asian Fold Belt (Buslov, 2011). These tectonic events are dated back to **380**–**324** Ma (Damdinov et al., 2018). During the Late Paleozoic tectonic-magmatic activation, the intrusion of dykes produced low-grade epithermal mineralization with predominate fahlores and, in some cases, Hg-bearing and telluride minerals (Airiyants et al., 2002).

So, our data on the age of the gold deposits discussed correspond to the main orogenic stage of the northern Central Asian Orogenic Belt.

5.2. Relation between gold mineralization and magmatism

All studied deposits and prospects are spatially associated with granitoid plutons, and the ore zones do not extend beyond their hosting granitoids. In some cases, quartz veins and veinlets are concentrated in the apical parts or in endocontacts of parental plutons. All studied deposits and prospects have undergone several stages of ore formation probably due to the cooling of the host granitoids. The gold deposits at the southeastern East Sayan typically contain high concentrations of gold pathfinder elements such as As, Sb, Bi and Te. Different mineral associations formed in different P-T conditions as well as the presence of As-Sb-Bi-Te(±Mo-W)-bearing mineral assemblages that are often observed in intrusion-related gold systems (Lang and Baker, 2000; Sillitoe and Thompson, 1998; Vikent'eva et al., 2019).

In some cases, the studied ore-hosting granitoids have an increased gold grade, e.g., as established at the Konevinskoye deposit (Damdinov et al., 2016). Moreover, accessory mineral assemblages from unaltered granites can include some gold-related minerals. In particular, at the Pogranichnoye prospect, accessory minerals are represented by native gold, silver, molybdenite and Au, Ag, Pb tellurides (Garmaev et al., 2013). Gold-telluride and gold-bismuth deposits are known to be often genetically associated with magmatic bodies that can be either intrusive (porphyry and gold-bismuth deposits) or volcanic (epithermal deposits) (Cook et al., 2009; Cooke et al., 2011; Goryachev and Gamyanin, 2006; Hedenquist et al., 1998; Krivtsov et al., 1986; Lang and Baker, 2001; Pak et al., 2006; Rowins, 2000; Seedorff et al., 2005; Sillitoe and Thompson, 1998; Vikent'eva et al., 2018). For gold-antimony deposits, this relationship is less obvious, but such deposits can form in connection with magmatic plutons (Bortnikov et al., 2010; Nevolko et al., 2018; Nevolko et al., 2019).

Oxygen isotope composition of the quartz in the studied intrusion-hosted deposits and prospects indicates that the gold mineralization was derived from a magmatic fluid. Estimated $\delta^{18}O$ values of the ore-forming fluids range from +5.7 to +7.4‰ in most cases. $\delta^{18}O$ values rarely deviate from magmatic values. $\delta^{18}O$ values of the ore-forming fluids in the Khoringolskoye prospect are +2.0 to +4.4‰. These data allow assumption of an admixture of meteoric waters in the magmatic fluid, which correlates with a relatively shallower depth of granitoid crystallization at this location. In addition, the calculated fluid isotopic composition of quartz-stibnite veins from the Tumannoye prospect shows relatively heavy oxygen ($\delta^{18}O$ = +8.2 to +8.9‰). Such values may indicate an addition of some metamorphic water in the later stages of ore formation. It corresponds to the geological setting of quartz-stibnite veins located in the fracture and schistosity zones in granodiorites where some dynamometamorphic processes occurred.

Comparison of the oxygen isotopic compositions in vein quartz with the quartz from ore-hosting granites in different types of deposits and prospects shows that all researched deposits have similar values of oxygen isotope fractionation factor between granite and the ore-forming fluid ($\Delta\delta^{18}O_{granite\text{-}fluid}$) from 2.35 to 2.8 (Table 4.)

It has been established that $\delta^{18}O$ values in the Pogranichnoye prospect consistently increase from hosting granites (11.3‰) through greisens (12.1‰) to quartz (12.9 – 14.3‰), which can be interpreted as a result of isotope fractionation during melt degassing and autometasomatism additionally providing relationships between quartz veins and hosting granites.

The data obtained on the oxygen isotope composition of the intrusion-hosted deposits significantly vary from orogenic gold deposits, e.g., Zun-Kholba, the largest gold deposit in the region. The fluid oxygen isotope composition calculated for this deposit shows values from 8.5 to 13.9‰; quartz $\delta^{18}O$ values are 12.4 – 17.8‰ (our unpublished data).

The sulfur isotope composition of the sulfide minerals of the intrusion-hosted deposits also testifies to its magmatic origin. Most $\delta^{34}S$ values in sulfides vary from −4.2 to 4.5‰, which corresponds to magmatic sulfur (Seal, 2006). Calculated values of $\delta^{34}S$ for the equilibrium ore-forming fluid correlate with juvenile (magmatic) sulfur. In most cases, $\delta^{34}S_{fl}$ values are close to zero. Only the Pogranichnoye prospect mineralization of the gold-bismuth-sulfosalt type are relatively enriched with "heavy" sulfur isotopes, with $\delta^{34}S$ values from 4.9 to 7.6‰. Such difference of these sulfides can be explained by the crustal nature of late orogenic parental granitoids, whereas other granitoids hosting gold mineralization have geochemical features of supra-subduction granites. Different types of such host granitoids vary in both trace-element distribution and K/Na ratios. Thus, granites with island arc geochemical features bear the lowest K/Na ratio of 0.42 – 0.45, while granites with continental arc geochemical characteristics

Table 4
Oxygen isotope fractionation factor between granite and the ore-forming fluid values.

Num.	$\Delta\delta^{18}O_{granite\text{-}fluid}$	Deposit/prospect
1	2.75	Konevinskoye
2	2.8	Sagangolskoye
3	2.75	Tumannoe
4	2.35	Pogranichnoye

have the intermediate ratio of 0.63 – 0.79 and late orogenic, post-subduction granites, the highest ratio of 1.38.

Thus, geological setting, stable isotope ratios, and mineralogy of the ores as well as geochemistry of the ore-hosting granitoids indicate the magmatic origin of the studied intrusion-hosted deposits. They significantly differ from the major orogenic gold deposits studied earlier in the region (Damdinov, 2019; Damdinov and Damdinova, 2018; Goldfarb et al., 2001, 2014; Gordienko et al., 2016; Goryachev and Pirajno, 2014). The largest orogenic deposits of the region (Zun-Kholba, Barun-Kholba, Zun-Ospa, Pioner et al.) are shown in Fig. 2. The ores of these deposits do not contain significant amounts of As-, Sb-, Bi-, and Te-bearing minerals. The main ore-forming minerals of such typical orogenic deposits are pyrite, chalcopyrite, galena, pyrrhotite, and sphalerite with minor amounts of native gold, rare Ag- and Sb-bearing sulfosalts. All this deposits are confined to shear and mélange zones often comprising a mixture of different rock fragments, e.g. gneisses, ophiolites, schists, granitoids, and carbonates (Damdinov and Damdinova, 2018; Zhmodik et al., 1993). Stable isotope composition of orogenic deposits reflects the metamorphic origin of the ore-forming fluids ($\delta^{18}O_{fl}$ up to 13.9‰). However, the studied intrusion-hosted deposits and prospects significantly differ from the "classical" orogenic gold deposits in several criteria: (1) geological setting; (2) ore morphology; (3) mineral composition; and (4) S-O isotope ratios, respectively. Those differences suggest a division of the orogenic gold deposits at East Sayan into "magmatic" and "metamorphic" subgroups. Based on our data, we propose a magmatic source for the hydrothermal fluids of the studied intrusion-hosted gold deposits.

5.3. A geodynamic model for formation of the ore-hosting granitoids

Geochemical characteristics of the studied ore-hosting granitoids correspond to granites formed in different geodynamic settings: island arc, continental arc, and orogenic (Damdinov et al., 2007, 2016, 2020a, b). On the Fig. 20 the concept models of probable tectonic settings of the formation of these granitoids is presented.

In the island arc setting, granitoid melt absorbed ore-forming elements come from a subducting slab and an overlying mantle wedge (Fig. 20a. As a result, the ores hosted in these granites acquire mantle isotopic characteristics, and a gold-telluride association emerges. Gold-telluride deposits and prospects of Neoproterozoic (~850 Ma) (Tainskoye) and Early Paleozoic (~500 Ma) (Khoringolskoye and Sagangolskoye) ages share many features and represent analogs. However, the Tainskoye deposit ores show more reducing and high-temperature formation conditions, which may be due to the greater depth of ore formation as well as to the older age of the deposit. Slightly different formation depths are assumed for the two above-mentioned prospects (Khoringolskoye and Sagangolskoye). This model is consistent with the suggestion that the telluride-bearing gold deposits formed in association with island arc granites (Goryachev, Pirajno, 2014, Mao at al., 2014; Sillitoe, Thompson, 1998 et al.).

Continental arc granitoids hosting gold-tetradymite and gold stibnite mineralization (Tannuol series) are formed in response to subduction of oceanic crust, enriched with gold and related elements (S, Cu, Zn), beneath the continental lithosphere (continental arc) or from slab dehydration under the continental crust in an orogenic setting (Fig. 20b. The resultant melt contained both mantle- (Te, Hg) and crust-derived (As, Sb, Pb, Bi, Mo, W, and partially S) elements. Such granitoids carrying Bi-Hg-Te- and Bi-Sb-bearing mineral assemblages, resulted in the formation of gold-tetradymite and gold-stibnite species of intrusion-hosted deposits represented by the Konevinskoye deposit and the Tumannoye prospect, respectively.

Formation of late-orogenic, post-subduction granites is due to melting during tectonic compression in the collision processes. The orogenic granites are enriched by crustal ore-forming components — Bi, As, Pb, Sb, W, and S (Fig. 20c. It leads to the formation of gold-bismuth-sulfosalt mineralization being associated with these granitoids. The orogenic granites hosting the Pogranichnoye prospect has specific mineralogical and isotopic characteristics differing from the other

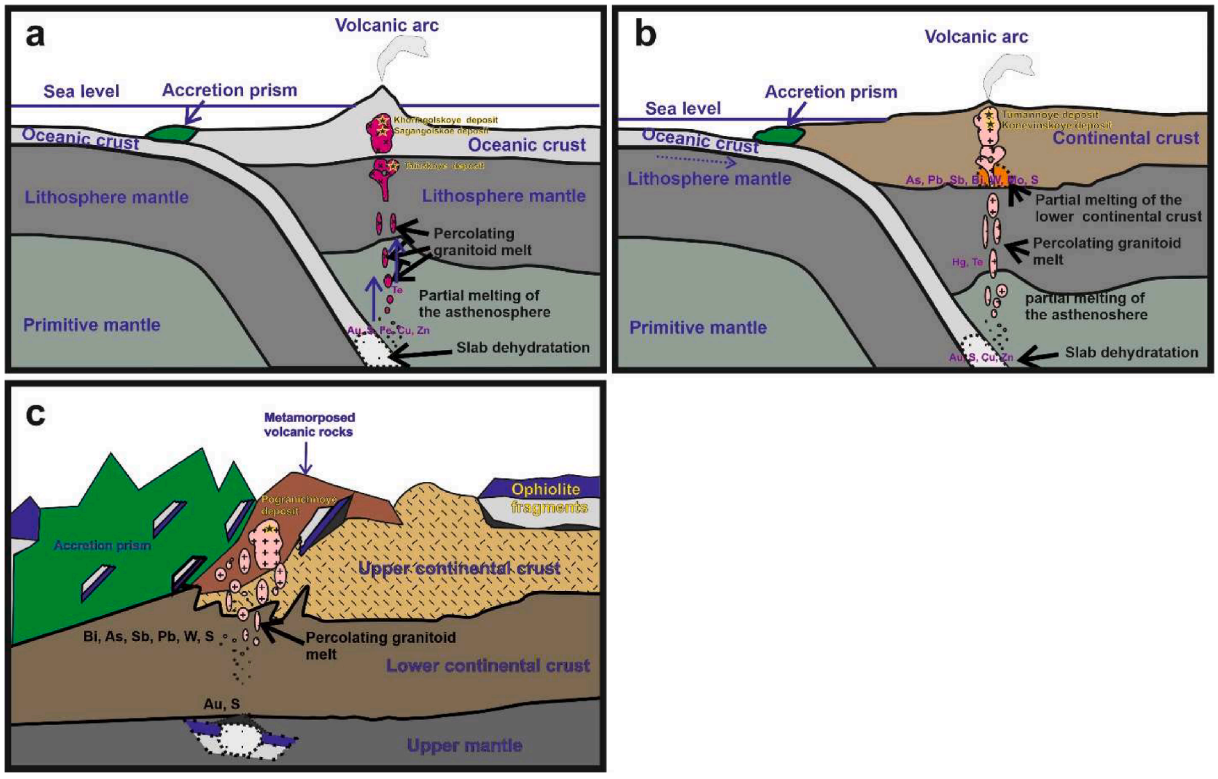

Fig. 20. Concept models of magma evolution and related gold mineralization in the southeastern part of the East Sayan. a – primitive (ensimatic – intraoceanic) island arc; b – continental arc; c – collision zone. For explanations, see the text.

studied deposits and prospects. Mantle and slab derived components (Te and Hg) occurring in the subduction arc-related granitoid hosting gold deposits are absent here, although rare microinclusions of tellurides are found in accessory parageneses, determining a small admixture of the mantle material. However, the mineralization of the gold-bismuth-sulfosalt type in the researched region has no economic significance.

6. Conclusions

1. We have studied intrusion-hosted gold deposits and prospects in the southeastern East Sayan. Geological setting, mineralogical, geochemical, and isotopic characteristics of the deposits indicate genetic relationships between gold mineralization and hosting granitoids. These characteristics allow differentiation of these deposits from major orogenic gold ones, formed by metamorphic ore-forming fluids.
2. On the basis of the main gold-bearing mineral assemblages, we recognize four different mineral assemblages of intrusion-hosted gold deposits: gold-telluride, gold-tetradymite, gold-stibnite, and gold-bismuth-sulfosalt. These deposits have some differences in the ore-hosting granitoid geochemistry.
3. Intrusion-hosted gold deposits were formed at two different orogenic periods during the geodynamic evolution of the northern part of the Central Asian fold belt. In the Neoproterozoic (about 850 Ma), gold-telluride deposits formed in association with late stage island arc granitoids. Subsequent Early Paleozoic mineralization (486–420 Ma) was associated with late stage orogenic activity reflecting the final phase of the Paleoasian Ocean evolution. At this time, different gold-bearing mineral assemblages formed in association with granitoids interpreted to be derived in island arc-, continental arc-, and orogenic settings, respectively.
4. The different gold-bearing mineral assemblages at southeastern East Sayan are interpreted by different compositions and tectonic settings of the host granitoids. Importantly, our data reveal that the subduction arc-related granitoids at East Sayan in the Central Asian Fold Belt are more likely to host economic gold mineralization.

Declaration of Competing Interest

The authors declare that they have no known competing financial interests or personal relationships that could have appeared to influence the work reported in this paper.

Acknowledgements

This work was supported by the Ministry of Science and Higher Education of the Russian Federation, GIN SB RAS (project AAAA-A21-121011390003-9, NEISRI FEB RAS (project number 121031700301-5), IGC SB RAS (project 0284-2021-0001), IGM SB RAS, and “CAS Hundred Talents Program” project (Y9CJ034000) to Xiao-Wen Huang. Authors acknowledge Peter Roschektayev for provided geological materials.

References

Airiyants, E.V., Zhmodik, S.M., Mironov, A.G., Borovikov, A.A., Borisenko, A.S., Ochirov, Y.C., 2002. Gold-mercury and gold-silver types of mineralization in East Sayan: mineral composition and physicochemical conditions of formation. Russ. Geol. Geophys. 43 (3), 273–285.

Anisimova I. V., Levitsky I. V., Salnikova E.B., Kotov A. B., Levitsky V. I., Reznitsky L. Z., Efremov S. V., Velikoslavinsky S. D., Barash I.G., Fedoseenko A.M. The age of the basement of the Gargan block (Eastern Sayan): results of U-Pb geochronological studies // Isotope systems and the time of geological processes (materials of the IV Russian conference on isotope geochronology). T. 1. Sankt-Peterburg, IGGD RAS, 2009, p. 35–36 (in Russian).

Bodnar, R.J., Vityk, M.O., 1994. Interpretation of microthermometric data for H_2O-NaCl fluid inclusions. In: De Vivo, B., Frezzotti, M.L. (Eds.), Fluid Inclusions in Minerals, Methods and Applications. Virginia Tech, Blacksburg, VA, pp. 117–130.

Borisenko, A.S., 1977. Study of the salt composition of solutions of gas–liquid inclusions in minerals by the cryometric method. Russ. Geol. Geophys. 18 (8), 16–27.

Bortnikov, N.S., Cramer, H., Genkin, A.D., Krapiva, L.Y., Santa-Cruz, M., 1988. Parageneses of gold and silver tellurides at the Florencia gold deposit, Cuba. Geol. Ore Deposits 2, 49–61.

Bortnikov, N.S., Gamynin, G.N., Vikent'eva, O.V., Prokof'ev, V.Y., Prokop'ev, A.V., 2010. The Sarylakh and Sentachan gold-antimony deposits, Sakha-Yakutia: a case of combined mesothermal gold-quartz and epithermal stibnite ores. Geol. Ore Deposits 52 (5), 339–372.

Brown, M., 2009. Metamorphic patterns in orogenic systems and the geological record. Geol. Soc. London. 318 (1), 37–74.

Buslov, M.M., 2011. Tectonics and geodynamics of the Central Asian Fold Belt: the role of late paleozoic large-amplitude strike-slip faults. Russ. Geol. Geophys. 52 (1), 52–71.

Coplen, T.B., 1988. Normalization of oxygen and hydrogen data. Chem. Geol. 72, 293–297.

Cook, N.J., Ciobanu, C.L., 2004. Bismuth tellurides and sulphosalts from the Larga hydrothermal system, Metaliferi Mts., Romania: Paragenesis and genetic significance. Mineral. Mag. 68 (2), 301–321.

Cook, N.J., Ciobanu, C.L., Spry, P.G., Voudouris, P., The participants of IGCP-486, 2009. Understanding gold-(silver)-telluride-(selenide) mineral deposits. Episodes, 32, 249–263.

Cooke, D.R., Deyell, C.L., Waters, P.J., Gonzales, R.I., Zaw, K., 2011. Evidence for magmatic-hydrothermal fluids and ore-forming processes in epithermal and porphyry deposits of the Baguio District, Philippines. Econ. Geol. 106, 1399–1424.

Damdinov, B.B., 2019. Mineral types of gold deposits and regularities of their localization in Southeastern East Sayan. Geol. Ore Deposits 61 (2), 118–132.

Damdinov, B.B., Garmaev, B.L., Mironov, A.G., Dashinimaev, Z.B., 2009. Gold-bismuth type of mineralization in the southeastern part of the East Sayan. Dokl. Earth Sci. 425 (1), 256–259.

Damdinov, B.B., Damdinova, L.B., 2018. Zun-Ospa gold deposit, Eastern Sayan: Geology, ore composition, and genesis. Geol. Ore Deposits 60 (3), 241–264.

Damdinov, B.B., Damdinova, L.B., Khubanov, V.B., Yudin, D.S., Travin, A.V., Buyantuev, M.D., 2020a. The tumannoe gold-antimony occurrence (East Sayan, Russia): mineralogy, fluid inclusions, S and O isotopes, and U-Pb and Ar-40/Ar-39 age. Geol. Ore Deposits 62 (3), 225–247.

Damdinov, B.B., Mironov, A.G., Borisenko, A.S., Guntypov, B.B., Karmanov, N.S., Borovikov, A.A., Garmaev, B.L., 2007. Composition and conditions of formation of gold-telluride mineralization in the Tissa-Sarkhoy gold-bearing province (East Sayan). Russ. Geol. Geophys. 48 (8), 643–655.

Damdinov, B.B., Zhmodik, S.M., Khubanov, V.B., Mironov, A.G., Travin, A.V., Damdinova, L.B., 2020b. Age and geodynamic conditions of formation for the Neoproterozoic gold-bearing granitoids in the Eastern Sayan. Geotectonics 54 (3), 356–365.

Damdinov, B.B., Zhmodik, S.M., Roshchektaev, P.A., Damdinova, L.B., 2016. Composition and genesis of the Konevinsky gold deposit, Eastern Sayan, Russia. Geol. Ore Deposits 58 (2), 134–148.

Damdinov, B.B., Zhmodik, S.M., Travin, A.V., Yudin, D.S., Goryachev, N.A., 2018. New data on the age of gold mineralization in the southeastern part of Eastern Sayan. Dokl. Earth Sci. 479 (2), 429–432.

Dobretsov, N.L., 1985. On the cover tectonics of the Eastern Sayan. Geotectonics 1, 39–50 [in Russian].

Dodson, M.H., 1973. Closure temperature in cooling geochronological and petrological systems. Contrib. Miner. Petrol. 40 (3), 259–274.

Fedotova, A.A., Khain, E.V., 2002. Tectonics of the South of the Eastern Sayan and Its Position in the Ural-Mongolian Belt. Scientific World, Moscow [in Russian].

Feofilaktov, G. A., 1970. About the genetic relationship of gold mineralization with granitoid massifs of the Kytoi-Urik ore cluster (Eastern Sayan). Ore-bearing capacity and structure of ore deposits of the Buryat Autonomous Soviet Socialist Republic. Proceedings of the Geology Department of Buryat Branch of the Siberian Branch of Academy of Science of USSR, vol.2 (10). Ulan-Ude. [in Russian].

Gao, J., Klemd, R., Zhu, M., Wang, X., Li, J., Wan, B., Xiao, W., Zeng, Q., Shen, P., Sun, J., Qin, K., Campos, E., 2018. Large-scale porphyry-type mineralization in the Central Asian metallogenic domain: a review. Ore Geol. Rev. 165, 7–36.

Garmaev, B.L., Damdinov, B.B., Mironov, A.G., 2013. Pogranichnoe Au-Bi occurrence, Eastern Sayan: composition and link to magmatism. Geol. Ore Deposits 55 (6), 455–466.

Goldfarb, R.J., Baker, T., Dubè, B., Groves, D.I., Hart, C.J.R., Gosselin, P., 2005. Distribution, character, and genesis of gold deposits in metamorphic terranes. Econ. Geol. 100, 407–450.

Goldfarb, R.J., Groves, D.I., Gardoll, S., 2001. Orogenic gold and geologic time: a global synthesis. Ore Geol. Rev. 18 (1-2), 1–75.

Goldfarb, R.J., Taylor, R.D., Collins, G.S., Goryachev, N.A., Orlandini, O.F., 2014. Phanerozoic continental growth and gold metallogeny of Asia. Gondwana Res. 25 (1), 48–102.

Gordienko, I.V., Roshchektaev, P.A., Gorokhovsky, D.V., 2016. Oka ore district of the Eastern Sayan: Geology, structural-metallogenic zonation, genetic types of ore deposits, their geodynamic formation conditions, and outlook for development. Geol. Ore Deposits 58 (5), 361–382.

Goryachev, N. A., Gamyanin, G. N., 2006. Gold-bismuth (gold-rare metal) deposits of the North-East of Russia: Types and prospects of industrial development. Proc. of the III All-Russian Symposium “Gold of Siberia and the Far East: Geology, Geochemistry, Technology, Economics, Ecology.” FEB RAS, Magadan, pp. 50-62. (in Russian).

Goryachev, N.A., Pirajno, F., 2014. Gold deposits and gold metallogeny of Far East Russia. Ore Geol. Rev. 59, 123–151.

Gvozdev, V.I., Grebennikova, A.A., Vakh, A.S., Goryachev, N.A., Fedoseev, D.G., 2020. Mineral Evolution during formation of gold-rare-metal ores in the Sredne-Golgotay Deposit (Western Transbaikalia). Russ. J. Pacific Geol. 39 (1), 70–91.
Hart, C.J.R., McCoy, D., Goldfarb, R.J., Smith, M., Roberts, P., Hulstein, R., Bakke, A.A., Bundtzen, T.K., 2002. Geology, exploration and discovery in the Tintina gold province, Alaska and Yukon. Soc. Econ. Geol. Spec. Publication 9, 241–274.
Hedenquist, J.W., Arribas Jr., A., Reynolds, T.J., 1998. Evolution of an intrusion-centered hydrothermal system: Far Southeast-Lepanto porphyry-epithermal Cu-Au deposits, Philippines. Econ. Geol. 93, 373–404.
Hodges, K.V., 2004. Geochronology and Thermochronology in Orogenic Systems // In: Treasure on Geochemistry. Oxford, UK: Elsevier, p. 263–292.
Hoefs, J., 2009. Stable Isotope Geochemistry, sixth ed. Springer-Verlag, Berlin Heidelberg, p. 285.
Hunger, R.B., Xavier, R.P., Moreto, C.P.N., Gao, J.-F., 2018. Hydrothermal alteration, fluid evolution, and Re-Os geochronology of the Grota Funda iron oxide copper-gold deposit, Carajas Province (Para State), Brazil. Econ. Geol. 113 (8), 1769–1793.
Khain, E.V., Bibikova, E.V., Kröner, A., Zhuravlev, D.Z., Sklyarov, E.V., Fedotova, A.A., Kravchenko-Berezhnoy, I.R., 2002. The most ancient ophiolite of the Central Asian fold belt: U-Pb and Pb-Pb zircon ages for the Dunzhugur Complex, Eastern Sayan, Siberia, and geodynamic implications. Earth Planet. Sci. Lett. 199 (3-4), 311–325.
Khubanov, V.B., Buyantuev, M.D., Tsygankov, A.A., 2016. U-Pb dating of zircons from PZ_3-MZ igneous complexes of Transbaikalia by sector-field mass-spectrometry with laser sampling: Technique and comparison with SHRIMP. Russ. Geol. Geophys. 57 (1), 190–205.
Kretschmar, U., Scott, S.D., 1976. Phase relations involving arsenopyrite in the system Fe-As-S and their application. Can. Mineral. 14, 364–386.
Krivtsov, A.I., Migachev, I.F., Popov, V.S., 1986. Copper-Porphyry Deposits of the World. Nedra. Moscow, 236 p. [in Russian].
Kuzmichev, A., Kröner, A., Hegner, E., Dunyi, L., Yusheng, W., 2005. The Shishkhid ophiolite, northern Mongolia: a key to the reconstruction of a Neoproterozoic island arc system in central Asia. Precambr. Res. 138 (1-2), 125–150.
Kuzmichev, A.B., 2015. Neoproterozoic accretion of the Tuva-Mongolian massif, one of the Precambrian terranes in the Central Asian Orogenic Belt. In: Kroner, A. (Ed.), The Central Asian Orogenic Belt: Geology, Evolution, Tectonics, and Models. Borntraeger Science Publishers, Stuttgart, pp. 66–92.
Kuznetsov, A.B., Letnikova, E.F., Vishnevskaya, I.A., Konstantinova, G.V., Kutyavin, E.P., Geletii, N.K., 2010. Sr chemostratigraphy of carbonate sedimentary cover of the Tuva-Mongolian microcontinent. Dokl. Earth Sci. 432 (1), 577–582.
Lang, J., Baker, T., 2001. Intrusion-related gold systems: the present level of understanding. Miner. Deposita 36 (6), 477–489.
Li, Y., Liu, J., 2006. Calculation of sulfur isotope fractionation in sulfides. Geochim. Cosmochim. Acta 70 (7), 1789–1795.
Mao, J., Pirajno, F., Lehmann, B., Luo, M., Berzina, A., 2014. Distribution of porphyry deposits in the Eurasian continent and their corresponding tectonic settings. J. Asian Earth Sci. 79, 576–584.
Mironov, A.G., Stein, H., Zimmerman, A., Zhmodik, S.M., 2005. Dating of gold occurrences in the Sayan-Baikal fold belt, Southern Siberia, Russia. In: Mao, J., Bierlein, F.P. (Eds.), Mineral Deposit Research: Meeting the Global Challenge. Springer Berlin Heidelberg, Berlin, Heidelberg, pp. 797–799.
Mironov, A.G., Zhmodik, S.M., 1999. Gold deposits of Urik-Kitoy metallogenic zone (Eastern Sayan, Russia). Geol. Ore Deposits 41 (1), 54–69.
Mironov, A.G., Zhmodik, S.M., Ochirov, Y.C., Borovikov, A.A., Popov, V.D., 2001. Tainskoye gold deposit (Eastern Sayan, Russia) – a new example of the porphyry gold type. Geol. Ore Deposits 43 (5), 353–370.
Nevolko, P.A., Pham, T.D., Fominykh, P.A., Tran, T.H., Tran, T.A., Ngo, T.P., 2019. Origin of the intrusion-related Lang Vai gold-antimony district (northeastern Vietnam): Constraints from fluid inclusions study and C-O-S-Pb isotope systematics. Ore Geol. Rev. 104, 114–131.
Nevolko, P.A., Pham, T.D., Tran, T.H., Tran, T.A., Ngo, T.P., Fominykh, P.A., 2018. Intrusion-related Lang Vai gold-antimony district (northeastern Vietnam): geology, mineralogy, geochemistry and $^{40}Ar/^{39}Ar$ age. Ore Geol. Rev. 104, 114–131.
Ohmoto, H., Rye, R.O., 1979. Isotope of sulfur and carbon. In: Barnes, H.L. (Ed.), Geochemistry of Hydrothermal Deposits. John Wiley & Sons, pp. 509–567.
Pak, S.J., Choi, S.-G., Oh, C.-W., Heo, C.-H., Choi, S.-H., Kim, S.-W., 2006. Genetic environment of the intrusion-related Yuryang Au-Te deposit in the Cheonan metallogenic province, Korea. Resour. Geol. 56 (2), 117–132.
Rowins, S.M., 2000. Reduced porphyry copper-gold deposits: a new variation on an old theme. Geology 28, 491–494.
Rudnev, S.N., Serov, P.A., Kiseleva, V., 2015. Vendian-Early Paleozoic granitoid magmatism in Eastern Tuva. Russ. Geol. Geophys. 56 (9), 1232–1255.
Rudnick, R.L., Gao, S., 2003. Composition of the continental crust, The Crust: Treatise on Geochemistry, Vol. 3 (ed. R. L. Rudnick et al.). Elsevier, 1–64.
Safonova, I.Y., Santosh, M., 2014. Accretionary complexes in the Asia-Pacific region: Tracing archives of ocean plate stratigraphy and tracking mantle plumes. Gondwana Res. 25 (1), 126–158.
Seal, R.R., 2006. Sulfur isotope geochemistry of sulfide minerals. Rev. Mineral. Geochem. 61 (1), 633–677.
Seedorff, E., Dilles, J.H., Proffett Jr., J.M., Einaudi, M.T., Zurcher, L., Stavast, W.J.A., Johnson, D.A., Barton, M.D., 2005. Porphyry deposits – characteristics and origin of hypogene features. Soc. Econ. Geol., Econ. Geol. 100th Anniversary Vol, 251–298.
Sharp, Z.D., Gibbons, J.A., Maltsev, O., Atudorei, V., Pack, A., Sengupta, S., Shock, E.L., Knauth, L.P., 2016. A calibration of the triple oxygen isotope fractionation in the SiO_2-H_2O system and applications to natural samples. Geochim. Cosmochim. Acta 186, 105–119.
Sillitoe, R.H., 2000. Gold-rich porphyry deposits: descriptive and genetic models and their role in exploration and discovery. SEG Rev. 13, 315–345.
Sillitoe, R.H., Thompson, F.H., 1998. Intrusion-related vein gold deposits: types, tectono-magmatic settings, and difficulties of distinction from orogenic gold deposits. Resour. Geol. 48 (2), 237–250.
Sun, S.S., McDonough, W.F., 1989. Chemical and isotopic systematics of oceanic basalts: implications for mantle composition and processes. In: Magmatism in the Ocean Basins, vol. 42.. The Geological Society, pp. 313–345.
Travin, A.V., Vladimirov, A.G., Tsygankov, A.A., Khanchuk, A.I., Ernst, R.E., Murzintsev, N.G., Mikheev, E.I., Khubanov, V.B., 2020. Thermochronology of the Angara-Vitim Granitoid Batholith, Transbaikalia, Russia. Doklady Earth Sci. 494 (1), 707–712.
Travin, A.V., Yudin, D.S., Vladimirov, A.G., Khromykh, S.V., Volkova, N.I., Mekhonoshin, A.S., Kolotilina, T.B., 2009. Thermochronology of the Chernorud granulite zone, Ol'khon Region, Western Baikal Area. Geochem. Int. 47 (11), 1107–1124.
Vikent'eva, O.V., Prokofiev, V.Y., Gamyanin, G.N., Goryachev, N.A., Bortnikov, N.S., 2018. Intrusion-related gold-bismuth deposits of North-East Russia: PTX parameters and sources of hydrothermal fluids. Ore Geol. Rev. 102, 240–259.
Yarmolyuk, V.V., Ivanov, V.G., Kovalenko, V.I., Pokrovskii, B.G., 2003. Magmatism and geodynamics of the Southern Baikal volcanic region (Mantle Hot Spot): results of geochronological, geochemical, and isotopic (Sr, Nd, and O) investigations. Petrology 11, 1–30.
Yarmolyuk, V.V., Kovalenko, V.I., Kovach, V.P., Rytsk, E.Y., Kozakov, I.K., Kotov, A.B., Sal'nikova, E.B., 2006. Early stages of the Paleoasian ocean formation: Results of geochronological, isotopic, and geochemical investigations of late Riphean and Vendian-Cambrian complexes in the Central Asian Fold Belt. Dokl. Earth Sci. 411 (1), 1184–1189.
Zhmodik, S.M., Dobretsov, N.L., Mironov, A.G., Roshchektaev, P.A., Karmanov, N.S., Kulikov, A.A., Nemirovskaya, N.A., Ochirov, Y.C., 1993. Mineralogical and geochemical signatures of hydrothermal-sedimentary origin of gold ore formation of the Kholba deposits, Eastern Sayan, Russia. Resour. Geol. Special Issue 17, 287–313.
Zhmodik, S.M., Mironov, A.G., Zhmodik, A.S., 2008. Gold-Concentrating Systems of Ophiolite Belts (on the Sayan-Baikal-Muya Belt Example). "Geo" Academic Publishing House, Novosibirsk, 304 p. [in Russian].
Zhmodik, S.M., Postnikov, A.A., Buslov, M.M., Mironov, A.G., 2006. Geodynamics of the Sayan-Baikal-Muya accretion-collision belt in the Neoproterozoic – early Paleozoic and regularities of the formation and localization of precious-metal mineralization. Russ. Geol. Geophys. 47, 187–201.